BMC Cancer

https://doi.org/10.1186/s12885-026-15650-x

Article in Press

Senogenic-senolytic treatment strategies enhance tumor control and can improve survival in murine cancer models: a systematic review

Received: 22 October 2025

Accepted: 22 January 2026

Published online: 31 January 2026

Cite this article as: Hamburger E.C., Brigato P., Rosenzweig D.H. *et al.* Senogenic-senolytic treatment strategies enhance tumor control and can improve survival in murine cancer models: a systematic review. *BMC Cancer* (2026). https://doi.org/10.1186/s12885-026-15650-x

Eleane C.B. Hamburger, Paolo Brigato, Derek H. Rosenzweig & Lisbet Haglund

Senogenic-senolytic treatment strategies enhance tumor control and can improve survival in murine cancer models: a systematic review

Eleane C.B. Hamburger[1,2], Paolo Brigato[3,4], Derek H. Rosenzweig[1,2,5] and Lisbet Haglund[1,2,3,6]*

Affiliations:

1. Department of Surgery, McGill University, Montreal, QC, Canada

2. Research Institute McGill University Health Centre, Montreal QC, Canada

3. Orthopaedic Research Laboratory, McGill University, Montreal, QC, Canada

4. Research Unit of Orthopaedic and Trauma Surgery, Department of Medicine and Surgery, Università Campus Bio-medico di Roma, via Alvaro del Portillo, Rome, Italy

5. Department of Orthopedic Surgery, University of Connecticut School of Medicine, Farmington, CT 06032, USA

6. Shriners Hospital for Children, Montreal QC, Canada

ORCID:

Eleane CB Hamburger: 0009-0006-0544-7102

Paolo Brigato: 0000-0002-8163-3787

Derek H Rosenzweig: 0000-0002-6593-8177

Lisbet Haglund: 0000-0002-1288-2149

***Corresponding author:** Lisbet Haglund, Department of Surgery, McGill University, Montreal, QC, Canada, Email: lisbet.haglund@mcgill.ca

Abstract

Background: Cellular senescence can be induced by therapeutic stress, contributing to tumor progression through the senescence-associated secretory phenotype (SASP). Senolytic drugs selectively eliminate senescent cells, offering a potential strategy to mitigate therapy-induced senescence (TIS) and improve cancer treatment outcomes. This review aimed to synthesize preclinical *in vivo* evidence evaluating the effects of senolytic and senogenic combination therapy on tumor burden and mechanistic outcomes, including senescence, SASP modulation, proliferation, apoptosis, and DNA damage markers.

Methods: Following PRISMA guidelines, a literature search was conducted using PubMed, Scopus, and Web of Science databases from inception to August 2025. Search terms included: *"senolytic drugs," "cellular senescence," "senescence clearance," "therapy-induced senescence," "senomorphic drugs," "chemotherapy," "cancer treatment," "in vivo,"* and *"xenograft," "PARP inhibitor," "CDK4/6*

inhibitor," "BCL-2 inhibitor," "BH3-mimetic," and "BET inhibitor". Eligible studies included *in vivo* cancer models evaluating senolytic + senogenic combinations compared with the_senogenic strategy alone, with outcomes related to tumor burden or mechanistic markers. Data extraction captured study design, animal model, tumor type, treatment regimen, and quantitative outcomes including senescence, SASP factors, proliferation, apoptosis, and DNA damage. Risk of bias was assessed using the SYRCLE tool for preclinical studies.

Results: The initial search identified 1,262 articles, of which 36 fulfilled the inclusion criteria after screening. All included studies were therapeutic mechanistic *in vivo* investigations. Across cancer types including colorectal, breast, ovarian, lung, melanoma, meningioma, prostate, head and neck, bladder, pancreatic, and hepatocellular carcinoma, senolytic co-treatment consistently reduced tumor burden compared with senogenic alone. Senescence markers such as SA-β-gal, p21, p53 and $p16^{INK4a}$ were decreased in the majority of combination groups, confirming attenuation of senescence-associated cell-cycle arrest. IL-6 was the most consistently suppressed SASP cytokine. Ki-67 was decreased and Caspase-3 activation increased across most models, supporting reduced proliferation and enhanced apoptosis. BCL2 downregulation and γ-H2AX elevation were observed in several studies, further suggesting increased apoptotic activity and DNA damage.

Conclusion: Senolytic plus senogenic combinations demonstrate robust preclinical efficacy in reducing tumor growth and senescent burden while promoting apoptosis across diverse *in vivo* models. These findings highlight senotherapy as a promising adjunct to conventional senescence-inducing anticancer therapies and underscore the need for standardized *in vivo* methodologies and translational studies to guide clinical application.

This review protocol was prospectively registered on PROSPERO (registration number: CRD420251161998).

Keywords: Cancer; cellular senescence; senolytics; SASP; therapy-induced senescence; in vivo models

1. Introduction

Cellular senescence is a state of stable cell cycle arrest induced by diverse stressors, including DNA damage, oxidative stress, and oncogenic signaling [1]. In the context of cancer therapy, modalities such as chemotherapy, radiotherapy, hormone-withdrawal approaches (e.g., castration), and targeted agents including PARP, and CDK4/6 inhibitors, frequently induce senescence in both malignant and stromal cells, and are therefore classified as senogenic treatments [2-6]. Although senescence can initially restrain tumor growth, the long-term accumulation of therapy-induced senescence

(TIS) may have deleterious consequences [2]. Senescent cells adopt a senescence-associated secretory phenotype (SASP) characterized by pro-inflammatory cytokines, chemokines, growth factors, and matrix-remodeling enzymes that can promote tumor proliferation, invasion, and resistance to therapy [7].

This dual role of senescence has driven interest in senotherapy, a strategy aimed at eliminating or modulating senescent cells to restore tissue homeostasis and mitigate SASP-driven tumor progression [8]. Senolytic agents selectively induce apoptosis in senescent cells by disrupting key survival pathways that sustain the senescent phenotype, including the anti-apoptotic BCL-2 family proteins (e.g., BCL-2, BCL-xL, MCL-1) and pro-survival signaling cascades such as PI3k/AKT and mTOR [8-10]. Senescence itself arises through activation of the DNA-damage response, engaging p53/p21 and $p16^{INK4a}$/Rb tumor-suppressor axes that enforce growth arrest while sustaining metabolic activity and SASP production via NF-κB and JAK/STAT3 pathways [10]. Preclinical studies demonstrate that combining senolytics with chemotherapy can interrupt these circuits reducing senescence markers (e.g., SA-β-gal, p21, $p16^{INK4a}$) and suppressing SASP cytokines (e.g., IL-6, IL-1α), thereby attenuating the tumor-promoting microenvironment and enhancing therapeutic efficacy [8, 11, 12].

Emerging preclinical evidence demonstrates that the SASP can reshape the tumor microenvironment and foster metastatic progression [9, 13, 14]. For example, senescent stromal cells induced by Carboplatin or Olaparib were shown to promote ovarian cancer cell growth and migration through paracrine signaling of SASP [15]. Similarly, in a model of head and neck cancer, Cisplatin-induced senescence conferred drug tolerance, whereas selective removal of senescent cells with the BCL-2 family inhibitor Navitoclax (ABT-263) delayed tumor growth and improved survival [16]. These findings, among others, underscore the ultimate effect of senescent cell accumulation and SASP as a possible target to reduce progression and recurrence of disease [14-17].

Senolytic therapies offer a novel strategy to mitigate the adverse effects of TIS [18]. Senolytic agents, such as Dasatinib and Quercetin, Fisetin, and BCL-2 inhibitors such as ABT-263, selectively induce apoptosis in senescent cells [19]; their use in preclinical cancer models has shown promise for removal of the senescent environment and reduction of disease burden [20]. For example, Dasatinib and Quercetin, when combined with Carboplatin or Olaparib, significantly reduced peritoneal and adipose tissue metastases in a model of ovarian cancer [15]. Likewise, Venetoclax synergized with Doxorubicin diminished senescence in a xenograft model aiding in reducing tumor burden [21]. Beyond reducing tumor load, clearance

of senescent cells has been linked to improved chemotherapy tolerance and decreased systemic toxicity [2, 11, 22].

Despite these advances, the application of senolytic and senogenic combinations remains at an early stage. Current evidence is derived primarily from animal studies and limited early-phase clinical trials. Many with a one-two hit strategy where the first hit is administration of a standard anticancer therapy, where senescence is induced, and the second hit is administering senolytics to target the induced senescent population [5, 23, 24]. Questions remain regarding optimal timing, dosing, and drug sequencing to maximize tumor suppression while minimizing off-target effects. Furthermore, given the heterogeneity of senescent phenotypes across tissues and tumor types, it is unclear which combinations will prove most effective and broadly applicable.

This systematic review, therefore, aims to synthesize the available evidence on senolytic and senogenic combinations in murine *in vivo* cancer models by focusing on tumor burden outcomes as well as mechanistic endpoints such as senescence, proliferation, and apoptotic markers. Clarification on whether senolytics consistently enhance the efficacy of standard anticancer therapies is still necessary due to the heterogenous nature of cancer and therapy-response specificity. Ultimately, this work aims to inform the

translational development of senolytic therapies as adjuvants in the context of oncological treatments.

2. Methods

2.1. Study Design and Protocol

This systematic review was conducted in accordance with the Preferred Reporting Items for Systematic reviews and Meta-Analyses (PRISMA) 2020 guidelines [25]. The protocol was designed to evaluate the efficacy of senolytic drugs in combination with senogenic treatment in *in vivo* murine cancer models. The research question was formulated according to the PICOS framework: Population (P): *in vivo* animal models of cancer, including xenograft, orthotopic, and syngeneic tumor-bearing rodents used to evaluate therapeutic efficacy; Intervention (I): combination therapy comprising senolytic or senomorphic agents co-administered with conventional senogenic (i.e., senescence-inducing anticancer therapy); Comparison (C): senogenic alone; Outcomes (O): quantitative measures of tumor burden, mechanistic endpoints of senescence, SASP markers, and downstream indicators of proliferation and apoptosis; Study design (S): preclinical *in vivo* experimental studies with comparator arms, assessing senolytic plus senogenic interactions through tumor and molecular outcomes, published in peer-reviewed journals (Table 1).

This systematic review protocol was prospectively registered on PROSPERO (registration number: CRD420251161998).

2.2. Search Strategy

A comprehensive literature search was conducted across PubMed, Scopus, and Web of Science, from database inception through August 2025, following PRISMA 2020 guidelines [25]. Search terms, linked by Boolean operators such as AND/OR, included: *"senolytic drugs," "cellular senescence," "senescence clearance," "therapy-induced senescence," "senomorphic drugs," "chemotherapy," "cancer treatment," "in vivo," and "xenograft," "PARP inhibitor," "CDK4/6 inhibitor," "BCL-2 inhibitor," "BH3-mimetic,"and "BET inhibitor".*

2.3. Eligibility Criteria

Inclusion and exclusion criteria are summarized in Table 1. Eligible studies were required to (1) include an *in vivo* murine model of cancer; (2) evaluate a senolytic or senomorphic agent administered in combination with a conventional senogenic anticancer strategy; (3) include a comparator arm (senogenic alone, senolytic alone, or vehicle control); and (4) report at least one quantitative tumor outcome (tumor volume, weight, or survival) and/or mechanistic endpoint related to senescence, SASP, proliferation, apoptosis, and/or DNA damage. Exclusion criteria comprised *in vitro* only studies, non-

cancer models, reviews, conference abstracts, case reports, editorials, and studies lacking a comparator arm or relevant outcome data.

2.4. Study Selection and Data Collection

Two independent reviewers screened (E.H. and P.B.) all records by title/abstract, followed by a full-text review of potentially eligible articles. Discrepancies were resolved by consensus, or by a third reviewer when necessary (L.H. or D.H.R.). From each study, the following information was extracted: first author, year of publication, country, cancer type, and cell line(s); animal model characteristics (species, strain, sex, implantation site, and group size); details of senolytic and senogenic agents (drug names, doses, routes, and treatment schedules); comparator arms (senogenic alone, senolytic alone, or control); primary tumor outcomes (tumor volume, weight, survival); and mechanistic endpoints related to senescence (e.g., SA-β-gal), SASP cytokines (e.g., IL-6), proliferation (e.g., Ki-67), and apoptosis or DNA damage (e.g., Caspase-3, γ-H2AX, BCL-2). Further, publication main findings and conclusions were gathered and reported.

2.5. Risk of Bias Assessment

Risk of bias was evaluated independently for each included study using the Systematic Review Centre for Laboratory Animal

Experimentation (SYRCLE) Risk of Bias tool, adapted from the Cochrane Collaboration framework for preclinical animal research [26]. The tool comprises ten domains addressing: (1) sequence generation, (2) baseline characteristics, (3) allocation concealment, (4) random housing, (5) blinding of investigators during intervention, (6) random outcome assessment, (7) blinding of outcome assessor, (8) completeness of outcome data, (9) selective outcome reporting, and (10) other potential biases (e.g., funding or conflicts of interest). Each domain was rated as “low risk” (+), “high risk” (–), or “unclear risk” (?) based on explicit information reported in the text, figures, or supplementary materials. When insufficient detail was provided, the item was marked “unclear.” Two reviewers assessed each study independently (E.H. and P.B.), with discrepancies resolved by discussion and consensus. A study-level summary score was not calculated; rather, domain-specific judgments were visualized in a SYRCLE summary chart to emphasize reporting quality and transparency. Studies were not assigned a composite numerical score. However, those with seven or more SYRCLE risk-of-bias domains rated as low risk were classified as overall low risk, those with four to six as moderate risk, and those with three or fewer as high risk of bias.

2.6. Data Synthesis

Data were synthesized only qualitatively due to heterogeneity in study design, animal models, drug combinations, and outcome reporting. Extracted quantitative outcomes, (i.e., tumor volume, tumor weight, and median survival), were summarized descriptively with values extracted directly from text, tables, or digitized figures where necessary. For mechanistic endpoints, directionality of change (↑, ↓, -, or NR) was recorded for markers of senescence (SA-β-gal, p21, p53, $p16^{INK4a}$), SASP cytokines (IL-6, IL-1α, IL-1β, TNF-α, IFN-γ), proliferation (Ki-67, PCNA), and apoptosis/DNA damage (Caspase-3, γ-H2AX, BCL-2, TUNEL). Results were grouped by cancer type to enable biological comparison across models. Where multiple xenograft lines were reported within a single study, each was considered a separate data point.

3. Results

3.1. Study Selection

A total of 1,262 records were identified through database searches. Following the removal of duplicates, 568 unique articles were screened by title and abstract. Studies were excluded if they were reviews, were exclusively *in vitro in nature*, or involved non-cancer or non-senolytic models. Sixty-three full-text articles were subsequently

assessed for eligibility, with twenty-seven excluded based on predefined criteria. Ultimately, thirty-six studies fulfilled all inclusion criteria and were incorporated into the qualitative synthesis. The complete study selection process is summarized in the PRISMA flow diagram (Figure 1).

3.2. Study Characteristics

Table 2 summarizes the characteristics of the studies that met the inclusion criteria [5, 6, 15, 16, 21, 27-57]. The included investigations evaluated senolytic or senomorphic agents in combination with a senogenic treatment across eleven cancer types: colorectal (n = 5), breast (n = 12), ovarian (n = 3), lung (n = 3), melanoma (n = 1), meningioma (n = 1), prostate (n = 3), head and neck (n = 2), bladder (n = 1), pancreatic (n = 3), and hepatocellular carcinoma (n = 2). All studies were *in vivo* therapeutic investigations. The majority employed human-derived xenograft models in immunodeficient mice, while twelve utilized syngeneic immunocompetent systems (CT26 colorectal [38]; MMTV-Wnt1 breast [39]; 4T1 breast [41, 43, 45, 46]; ID8-luc ovarian [15]; B16 melanoma [50]; MycCaP prostate [53]; OSCC-602 head and neck [16]; Panc02 pancreatic [56]; L1475luc lung [49]). Tumor implantation was performed subcutaneously in 25 studies, while four study used orthotopic mammary-fat-pad implantation [31, 39, 41, 42], and one used intraperitoneal injection

[15]. Group sizes ranged from 3 [41] to 20 [31] animals per arm, and treatment durations varied between 2 [5, 29, 45, 46] and 8 weeks [16, 34].

3.3. Interventions, Routes and Dosages

Dosing regimens and routes of administration for senogenic and senotherapeutic agents are summarized in Table 3. A range of senogenic plus senolytic combinations were evaluated across studies. Senogenic agents included Doxorubicin, Talazoparib, Palbociclib, Irinotecan, 5-Fluorouracil, Leucovorin, Fulvestrant, Etoposide, ionizing radiation, Cyclophosphamide, Olaparib, Carboplatin, Docetaxel, Cisplatin, Everolimus, Gemcitabine, Mitoxantrone, androgen-deprivation via surgical castration, LY2835219 (Abemaciclib), Mitomycin C, and nab-Paclitaxel (Abraxane). Senolytic and senomorphic agents comprised ARV825 (BET degrader), α-PD-L1 antibody, Artesunate, Atorvastatin, Navitoclax (ABT-263), GALNP-Navitoclax, Nav-Gal, Venetoclax, Nifuroxazide, Caulerpin, Curcuma-derived extracellular vesicles with death receptor 5 agonist, IQ-NPs (Quercetin + IR1061 NIR-II nanoparticles), Quercetin, Dasatinib, Dasatinib + Quercetin (D+Q), Rosiglitazone, ABT-737, mGL392, Procyanidin C1, S63845, Metformin, Integrin α2β1 ligand peptide (TFA), HCW9218, and Ganoderma lucidum triterpenoid complex. Senogenic therapies were delivered predominantly by the

intraperitoneal route (61%) [5, 15, 16, 21, 27, 29-31, 33, 34, 36, 37, 39, 40, 42, 47, 49, 51, 52, 55-57], followed by oral administration (25%) [6, 38, 40, 41, 43, 44, 50, 51, 54]. Two studies employed an *in vitro* irradiation-based senescence protocol, in which tumor cells were pre-treated with Talazoparib for 72 hours and exposed to 6 Gy prior to injection [45, 46]. Three studies used intravenous delivery for the senogenic agent [32, 35, 48], one employed external laser exposure [6] and another employed androgen-deprivation through castration [53] as part of the treatment protocol. Senolytic and senomorphic agents were most commonly administered orally (47%) [5, 16, 21, 39, 40, 42, 44-46, 48-53, 56, 57], followed by intraperitoneal injection (44%) [15, 29-31, 33, 34, 37, 38, 41, 43, 44, 47, 49, 50, 54, 55]. Three studies used intravenous senolytic delivery [6, 32, 35], and one used subcutaneous dosing [36]. One study did not report the administration route [28].

Combination regimens varied across cancer types. Representative examples include: colorectal cancer: Irinotecan (75mg/kg) combined with Artesunate (30mg/kg); breast cancer: Doxorubicin (1.5mg/kg) with Venetoclax (50mg/kg) [21]; ovarian cancer: Carboplatin (2mg/kg) or Olaparib (50mg/kg) with Dasatinib (5mg/kg) and Quercetin(50mg/kg) [15]; lung cancer: Etoposide (12mg/kg) with ABT-737 (100mg/kg) [47]; melanoma: Palbociclib (2.5mg/kg) with mGL392 (0.015mg/kg) and/or Quercetin (1.25mg/kg) and/or Dasatinib

(0.125mg/kg) [50]; meningioma: Everolimus (2mg/kg) plus Gemcitabine (10mg/kg) with Navitoclax (100mg/kg) [51]; prostate cancer: Mitoxantrone (0.2mg/kg) with Procyanidin C1 (20mg/kg) [34]; head and neck cancer: Cisplatin (5mg/kg) with Navitoclax (80mg/kg) [16]; bladder cancer: Mitomycin C (5mg/kg) with Integrin α2β1 ligand peptide TFA (2.5mg/kg) [35]; pancreatic cancer: Gemcitabine (40mg/kg) and nab-Paclitaxel (50mg/kg) combined with HCW9218 (3mg/kg) [36]; and hepatocellular carcinoma: Doxorubicin (6mg/kg) with Ganoderma lucidum triterpenoid complex TC (100 or 250mg/kg) [37].

3.4. Risk of Bias within Studies

Risk of bias was assessed using the SYRCLE tool [26] (Figures 2 and 3)**.** Across the assessed domains, reporting was frequently incomplete. Random sequence generation and allocation concealment were seldom described. Baseline characteristics were generally comparable between groups, but blinding of caregivers and outcome assessors was almost uniformly unclear. Selective outcome reporting was considered to present a low-to-moderate risk of bias in most studies. Within the other bias domain, additional methodological limitations were identified. Several studies did not include an appropriate vehicle-treated control group, which constrained interpretation of whether observed effects could be attributed to the

investigational agents rather than baseline variability [34, 41, 51]. In other studies, inconsistencies in measurement timing or insufficient justification for differing sampling intervals introduced uncertainty when comparing tumor burden across groups [48]. A small number of manuscripts also exhibited reporting or figure-level inaccuracies, including mislabelled drug concentrations [46], reducing confidence in the precision of the presented data. Collectively, these factors contributed to several studies being rated as high risk in the other bias domain.

3.5. Tumor Burden and Survival Outcomes

Reported tumor and survival outcomes are summarized in Table 4. All included studies assessed tumor burden using at least one quantitative endpoint (i.e., tumor volume, tumor weight, or survival), comparing combination therapy (senogenic plus senolytic) to senogenic alone. Across cancer types, co-treatment consistently enhanced tumor suppression relative to senogenic alone, indicating a reproducible therapeutic advantage of combination regimes *in vivo.*

3.5.1. *Tumor Volume*

Tumor volume was the most frequently reported outcome, evaluated in thirty-five studies using caliper-based calculations (e.g., $V = L \times W^2 / 2$), and in one study via bioluminescence imaging [15]. Among the

thirty-five studies providing numerical or graphical data, tumor volume was reduced in the combination group in 97% of cases, with decreases commonly ranging from approximately 40% to over 80% relative to senogenic alone. One study reported no additional reduction in tumor size with senolytic co-treatment; however, mechanistic analyses demonstrated increased apoptotic activity and reversal of Cyclophosphamide-induced ovarian toxicity, indicating therapeutic benefit beyond gross tumor shrinkage [31].

3.5.2. Tumor Weight

Tumor weight was reported in ten studies and closely parallelled the tumor volume trends. In most cases, combination-treated groups exhibited lower tumor weights compared with senogenic treatment across colorectal [28-30], breast [32, 39, 43], head and neck [54], and hepatocellular carcinoma [37, 57] models, with reductions ranging from approximately 30% to 90% relative to senogenic treatment alone. One study reported tumor-burden values that were comparable between the senogenic and combination groups, indicating no additional reduction [56]. Overall, 9 of the 10 studies (90%) that reported tumor weight demonstrated lower tumor weights with combination therapy, further supporting an enhanced tumor-suppressive effect of senolytic co-administration across diverse cancer types.

3.5.3. Survival

Survival outcomes were assessed in nine studies, all of which demonstrated improvement with combination treatment. Across colorectal [38], breast [39-41], prostate [34, 53], head and neck [16], bladder [35], and pancreatic cancer [36] models, combination therapy extended survival relative to senogenic treatment alone. Reported gains ranged from modest improvements of approximately 4-9% [35, 36] to intermediate increases of roughly 20-40% [38-41], and to

substantial extensions exceeding 40% [16, 34, 53]. Notably, no study observed decreased survival in the combination group, reinforcing the potential of senolytic co-administration to enhance therapeutic durability without compromising safety.

3.6. Mechanistic Outcomes

Mechanistic outcomes were reported in thirty-one studies, encompassing biomarkers of senescence, SASP cytokines, proliferation, apoptosis, and DNA damage (Table 5). These endpoints were assessed using histological and molecular approaches, including senescence-associated β-galactosidase (SA-β-gal) staining, hematoxylin and eosin (H&E) staining, immunohistochemistry, immunofluorescence, Western blotting, and quantitative PCR or ELISA for SASP cytokines. Five studies [5, 33, 47, 48, 55], met inclusion criteria as *in vivo* therapeutic investigations and were retained based on their quantitative tumor-outcome data, although they did not report mechanistic endpoints. They are therefore designated “NR” for mechanistic measures in Table 5.

3.6.1. *Senescence*

SA-β-gal, a histochemical marker of lysosomal β-galactosidase accumulation in senescent cells, was reduced in thirteen out of the thirty-six models, confirming effective clearance of senescent cells

[15, 16, 21, 28-30, 34, 35, 37, 38, 49, 50, 52]. With one study showing no significant change in SA-β-gal [57]. Downregulation of p21 and p53 was observed across colorectal, breast, ovarian, prostate, pancreatic and hepatocellular carcinoma models, indicating attenuation of senescence-associated cell-cycle arrest pathways [27-31, 34, 36, 37, 44, 49]. Further evidence was seen with six studies demonstrating *in vivo* reductions of $p16^{INK4a}$ expression by immunohistochemistry, immunofluorescence or Western blot [28, 29, 32, 34, 37, 52]. Given its role as a key regulator of the $p16^{INK4a}$-Rb axis, $p16^{INK4a}$ suppression supports the functional elimination of senescent cells. In contrast, senomorphic agent Nifuroxazide in combination with Palbociclib elevated p21 [43], supporting the classification of senomorphics to attenuate SASP but not senescent cells. Together, these findings demonstrate that combination treatment with senolytics effectively decreases senescent cell burden *in vivo*, potentially restoring proliferative homeostasis and enhancing senogenic response.

3.6.2. SASP

Among SASP mediators, IL-6 was most frequently measured (8/36 studies) and consistently suppressed across colorectal, breast, prostate, pancreatic and hepatocellular carcinoma models [28-30, 32, 34, 36, 37, 43]. IL-1α was decreased in breast, prostate, pancreatic and hepatocellular carcinoma models [34, 36, 37, 43], while IL-1β was

decreased in six models spanning colorectal, breast, prostate and hepatocellular carcinoma models [28-30, 34, 37, 43]. TNF-α was decreased in three colorectal [28-30] and in one breast [43] model. In contrast, IFN-γ was reported increased in two studies, breast [32], and pancreatic [36] suggesting selective enhancement of immune activation alongside SASP suppression. Among less frequently reported mediators, IL-8 was reported decreased in a single prostate model [34]; this isolated finding aligns with the broader trend of SASP suppression but was not included in Table 5 due to limited reporting. Together, these data demonstrate consistent downregulation of pro-inflammatory SASP signalling and limited activation of immune-stimulatory pathways following combination therapy.

3.6.3 Proliferation, Apoptosis and DNA damage

Proliferation markers were broadly decreased: Ki-67 was reduced across thirteen models of colorectal, breast, lung, prostate, head and neck, pancreatic, and hepatocellular carcinoma [6, 16, 21, 28-30, 37, 40, 43, 49, 52, 54, 56]. PCNA was decreased in three colorectal models [28-30], and one head and neck [54], indicating reduced tumor cell proliferation with combination therapy. Apoptotic activity was enhanced, evidenced by increased cleaved Caspase-3 expression in fifteen out of thirty-six models [16, 27-30, 34, 35, 39-42, 50-53]. In several models, γ-H2AX, a marker of DNA double-strand breaks, was

either increased [27, 34], decreased [29], or unchanged relative to senogenic alone [16, 56], reflecting variable degrees of DNA-damage signaling among models. The anti-apoptotic protein BCL-2 was downregulated in colorectal [28-30], and prostate [52] models, supporting increased apoptotic sensitivity to therapy. TUNEL positivity was seen increased in breast [44-46], lung [49], and hepatocellular carcinoma [37] models, indicating enhanced apoptotic DNA fragmentation consistent with greater clearance of damaged or senescent tumor cells under combination treatment. CD49 expression was elevated in a breast cancer model [32], potentially reflecting enhanced cell-matrix or extracellular-vesicle interactions; this single observation was not included in Table 5 due to isolated reporting.

Collectively, these findings indicate that combination therapy consistently suppressed senescence and SASP activity while enhancing apoptotic and DNA-damage responses, correlating with reduced tumor burden across diverse *in vivo* cancer models.

3.7. Toxicity and Risk Profile Data

Toxicity outcomes were variably reported across the included *in vivo* studies (Table 6). None described treatment-related mortality or systemic toxicity attributable to combination therapy. Body weight was the most consistently evaluated indicator of tolerability and remained stable in the majority of models which it was assessed. In

colorectal studies, combination treatment maintained or slightly increased body weight and reduced chemotherapy-induced diarrhea, reflecting improved gastrointestinal tolerance [28-30]. In a breast cancer model, hematologic parameters remained within normal limits and body weight was preserved across treatment groups, with several studies explicitly reporting no abnormalities in liver, kidney, or spleen histology [32, 39, 43]. Further, Caulerpin co-treatment mitigated Cyclophosphamide-induced weight loss and alleviated ovarian toxicity [31]. While weight loss was reversed at the systemic level, ovarian protection was mediated via suppression of p53/NF-kB-driven macrophage polarization and ROS-driven granulosa-cell senescence, restoring follicle counts and serum AMH and FSHR expression [31]. Death Receptor 5 (DR5) targeted Curcuma extracellular vesicles (EVs) combined with Doxorubicin showed excellent biosafety, while Venetoclax plus Doxorubicin caused no significant weight change [21, 31, 32]. Ovarian cancer models demonstrated stable body weight (~21–23 g) and no abnormal clinical signs across treatment groups [15]. In prostate cancer, hematologic and histologic assessments confirmed normal blood counts and preserved liver, kidney, and spleen architecture, indicating systemic safety [34]. In head and neck models, showed stable body weight and no hematologic toxicity, with platelet and neutrophil counts remaining within physiological ranges [16, 54]. Several lung cancer, melanoma, and pancreatic cancer

studies also reported stable body weight and normal organ histology, with no evidence of systemic or hematologic toxicity [48-50, 55]. No toxicity data were reported in bladder or some pancreatic and hepatocellular carcinoma models [35, 36]. However, in one of the hepatocellular carcinoma models, the addition of a triterpenoid complex to Doxorubicin normalized serum alanine aminotransferase (ALT), aspartate aminotransferase (AST), and creatinine levels and restored body weight, indicating reversal of Doxorubicin-induced hepatotoxicity and renal stress [37]. Across all models with available data, combination treatment did not exacerbate senogenic-related toxicity; rather, several studies demonstrated protective or toxicity-mitigating effects [28-32, 37]. Collectively, these findings suggest that senolytic co-administration may enhance systemic tolerability while maintaining or improving therapeutic efficacy.

Overall key results and clinical applicability are explicitly summarized in Table 7.

4. Discussion

4.1. Background and Main Findings

This systematic review synthesized thirty-six *in vivo* studies evaluating senotherapeutic agents in combination with senogenic therapies across diverse tumor types. Most models demonstrated

benefit: tumor volume decreased with combination treatment in approximately 95% of comparisons, tumor weight in approximately 90% of studies reporting this outcome, and all nine studies reporting survival showed extensions relative to senogenic therapy alone. Several breast and prostate models additionally reported reduced metastatic burden or delayed relapse [41, 43, 44, 52], and bladder and pancreatic studies demonstrated improved survival even without explicit metastasis measurements [35, 36].

Despite these encouraging trends, the magnitude and durability of response varied considerably. Some regimens produced deep and sustained tumor control, including complete remissions in colorectal cancer [38], whereas others resulted in only modest or transient improvements [40, 53, 56], or no measurable benefit in specific tumor contexts [57]. Notably, although chemotherapy-or radiation-induced senescence is common in cancer models, the resulting senescent tumor populations do not uniformly respond to senolytic agents. Senolytic sensitivity can differ substantially by tumor lineage, the senescence-inducing stimulus, and/or the survival pathways activated [58].

This variability is further illustrated by reports outside our inclusion set showing that certain therapy-induced senescent tumor cells (e.g., LNCaP prostate cancer) are refractory to canonical senolytics,

preventing progression to *in vivo* evaluation [59]. In LNCaP cells, senescence triggered by androgen receptor modulation (R1881 or Enzalutamide) remained resistant to Navitoclax, a BCL-2/BCL-xL inhibitor, despite robust p21/p16 induction, and was similarly unresponsive to MK2206 or Ganetespib. These findings demonstrate that senolytic susceptibility is strongly shaped by the senescence trigger and the cell-intrinsic survival programs engaged [59, 60], helping to explain why agents effective against age-related senescent cells show inconsistent activity in cancer TIS models.

Collectively, this body of evidence provides an essential counterbalance to the *in vivo* literature. While eliminating or modulating senescent cells can markedly improve tumor control and, in some cases, reduce metastasis, therapeutic efficacy is highly context- and agent-dependent. Senolytics developed for age-related pathologies do not uniformly translate to cancer-therapy-induced senescence, underscoring the necessity for mechanistic validation of senescence programs and survival dependencies when selecting senotherapeutic combinations for preclinical or translational application.

4.2. Establishment of Senescence and Early Oncologic Applications

Cellular senescence, a stable growth-arrest response to DNA damage or oncogenic signaling, was initially viewed as a tumor-suppressive

barrier [61]. Subsequent evidence revealed that TIS can paradoxically drive tumor relapse through the pro-inflammatory SASP [7, 62, 63]. Early studies in nasopharyngeal and breast cancer models treated with Cisplatin or Doxorubicin showed that residual senescent cells persisted after therapy and promoted regrowth [64-66].

The development of senolytic drugs such as Dasatinib + Quercetin (D+Q) and Navitoclax (ABT-263) demonstrated that selective clearance of senescent cells can restore tissue function and improve therapeutic response *in vivo* [67, 68]. In the thirty-six studies included in this review, co-administration of senolytics with chemotherapy consistently reduced senescence markers (SA-β-gal, p21, p53, $p16^{INK4a}$) and tumor burden across diverse cancer types. Regardless of mechanism, whether via BCL-2 inhibition (Venetoclax, ABT-263) or SASP modulation (Atorvastatin, Artesunate), these combinations yielded similar benefits, underscoring that elimination of senescent cells rather than targeting a single signaling pathway is the key determinant of efficacy. Similarly*, in vitro*, co-treatment with senolytics o-Vanillin and RG-7112 alongside Doxorubicin reduced senescence and overall tumor cell proliferation in a model of breast cancer, reinforcing the therapeutic rationale for combining senolytic and chemotherapeutic strategies [69].

4.3. Senescence Beyond Oncology

Beyond oncology, the biological rationale for senescence clearance extends to other age- and stress-related disorders. Insights gained from cancer models have guided investigations of senolytics in cardiovascular, neurodegenerative, and musculoskeletal diseases, emphasizing the broader therapeutic potential of targeting the senescent cell population [70-73].

Senolytic interventions have shown functional improvement in multiple non-cancer models such as Dasatinib + Quercetin improving frailty and physical function in aged mice, also proving that senolytics could potentially offer effects that persist weeks post discontinuation of treatment [73]. Further, Navitoclax has shown that clearing senescent astrocytes can alleviate neuroinflammation in Alzheimer's models [71], and o-Vanillin, RG-7112 and Fisetin are example senolytics that have shown reduction in intervertebral disc degeneration in *ex vivo* and *in vivo* models [70, 72]. These parallels highlight that senescence-targeted therapies hold promise across diverse diseases, with oncology serving as a leading, but not exclusive area of clinical application.

4.4. Clinical Translation and Future Direction

Senolytic therapy is rapidly advancing from concept to clinic. Senolytic combination of Dasatinib + Quercetin has reached human

trials for idiopathic pulmonary fibrosis (NCT02874989), and diabetic kidney disease (NCT02848131), where intermittent dosing reduced senescence biomarkers such as $p16^{INK4A}$ and circulating SASP cytokines [74, 75]. In oncology, early-phase studies are testing Navitoclax (ABT-263) in recurrent epithelial ovarian cancer (NCT02591095) [76] and in cases of myelofibrosis in combination with standard treatment Ruxolitinib (NCT03222609) [77]. The Dasatinib + Quercetin regimen in combination with immune checkpoint blockade for head and neck squamous cell carcinoma is also under investigation having just concluded phase II (NCT05724329) [78]. Current recruitment is being staged for a Phase II clinical trial to evaluate Dasatinib + Quercetin treatment to reverse chemotherapeutic resistance in triple-negative breast cancer (NCT06355037).

Venetoclax, another clinically approved BCL-2 inhibitor, is under active investigation in phase I/II trials for multiple malignancies, including acute myeloid leukemia (NCT03672695) [79], and solid tumor combinations (NCT04029688). These ongoing efforts mirror the preclinical results synthesized here, in which BCL-2–targeting senolytics enhanced chemotherapy-induced apoptosis and attenuated SASP signaling across tumor types.

Future research could investigate standardization of senescence and SASP marker panels, utilize immunocompetent or orthotopic models, and define optimal timing for senolytic administration relative to senogenic testing across the same cancer model.

4.5. Limitations

Although all included studies met the inclusion criteria for *in vivo* design, heterogeneity among the thirty-six models spanning colorectal, breast, ovarian, lung, melanoma, meningioma, prostate, head and neck, bladder, pancreatic, and hepatocellular carcinoma limited quantitative meta-analysis. Variability in animal strain, treatment duration, and senolytic dosing constrained direct comparison of results. Most studies used immunodeficient xenograft systems, preventing assessment of immune-mediated senescent-cell clearance. Inconsistent toxicity and survival reporting, along with partial SASP profiling, also reduced cross-study comparability. Potential limitations of the review process include dependence on reported data that could not be independently validated, potential omission of non-English publications, and exclusion of unpublished or negative studies.

5. Conclusion

Across thirty-six *in vivo* models, senolytic plus senogenic combinations generally improved tumor suppression while maintaining an acceptable safety profile. These findings support senescence-targeted strategies as a promising adjunct to conventional cancer therapies, with the potential to mitigate therapy-induced senescence and SASP-driven tumor progression. However, responses were variable across tumor types and senescence-inducing stimuli, underscoring that senolytic efficacy is not uniform and remains highly context dependent. Further progress will require mechanistic refinement of senolytic agents, clearer understanding of survival dependencies in therapy-induced senescence, and careful integration with immunomodulatory approaches. Ultimately, whether this “one-two punch” strategy can translate into clinically meaningful benefit will depend on rigorous biomarker development, rational patient selection, and validation in prospective translational studies.

List of abbreviations

3D = three-dimensional

ARV-825 = BRD4-targeting senolytic degrader

BCL-2 = B-cell lymphoma 2

Caul = Caulerpin

Curc-EVs = Curcumin-loaded extracellular vesicles

DOX = Doxorubicin

γ-H2AX = Phosphorylated histone H2AX

HCC = hepatocellular carcinoma

IL = interleukin

SA-β-gal = senescence-associated β-galactosidase

SASP = senescence-associated secretory phenotype

SYRCLE = Systematic Review Centre for Laboratory Animal Experimentation

TIS = therapy-induced senescence

VEN = Venetoclax

Cell line abbreviations:

HCT116 = Human colorectal carcinoma

CT26 = Murine colorectal carcinoma

4T1 = Murine triple-negative breast carcinoma

MDA-MB-231 = Human breast adenocarcinoma

MCF-7 = Human breast carcinoma

MMTV-Wnt1 = Spontaneous murine mammary tumor model

PDX315, 1232, 1105 = Patient-derived breast cancer xenografts

A2780, SKOV3 = Human ovarian carcinoma

ID8-luc = Luciferase-tagged murine ovarian carcinoma

OV4453, 1946 = Human ovarian carcinoma

A549 = Human lung adenocarcinoma

SW1573 = Human non-small lung carcinoma

NCI-H1650 = Human lung adenocarcinoma

LX22, 36 = Patient-derived small cell lung carcinoma

L1475-luc = Luciferase-expressing lung carcinoma

B16 = Murine melanoma

IOMM-Lee = Human malignant meningioma

PC3 = Human prostate carcinoma

PSC27 = Prostate stromal cells

PC3 Luc-shTIMP1 = Luciferase-expressing PC3 with TIMP1 knockdown

MycCaP = Murine prostate carcinoma

OSCC-602 = Oral squamous cell carcinoma derived from 4NQO model

HSC6 = Human oral squamous carcinoma

T24 = Human bladder carcinoma

SW1990, AsPC1 = Human pancreatic carcinoma

Panc02 = Murine pancreatic adenocarcinoma

eqFP650-Huh-7 = Fluorescent human hepatocellular carcinoma

HepG2 = Human hepatocellular carcinoma

Animal models:

BALB/c = Immunocompetent inbred mouse strain

NOD/SCID = Non-obese diabetic severe combined immunodeficient mouse

C57BL/6 = Immunocompetent inbred mouse strain

Athymic nude = T-cell–deficient nude mouse

SCID = Severe combined immunodeficient mouse

NSG = NOD SCID IL2R gamma$^{-/-}$ mouse (lacks T, B, and NK cells)

NRG = NOD Rag gamma mouse (lacks T, B, and NK cells)

FVB/N = Immunocompetent inbred mouse strain used in transgenic and tumor models

Implantation and administration routes:

s.c. = Subcutaneous

i.p. = Intraperitoneal

i.v. = Intravenous

orthotopic = Implantation into the original organ site

trocar = Trocar-assisted transplantation

Declarations

Ethical approval and consent to participate: Not required.

Consent for publication: Not applicable.

Availability of data: All data generated or analysed during this study are included in this published article.

Competing interests: The authors declare no conflicts or competing interests.

Funding: Funding for this work was obtained from The Cancer Research Society Operating Grants 2022 [#944456] awarded to DHR and LH.

Acknowledgements: We are thankful for the continued support from the McGill Scoliosis and Spine Group. ECBH received and is thankful for the fellowships from the Research Institute of McGill University Health Centre.

Author contributions: Project conception: ECBH, DHR and LH. Data collection: ECBH and PB. Data analysis: ECBH and PB. Funding

acquisition: LH and DHR. Manuscript draft: ECBH. All authors contributed to manuscript editing and final review.

Trial registration: Clinical trial number: not applicable.

References

1. Ajoolabady, A., et al., *Hallmarks of cellular senescence: biology, mechanisms, regulations.* Exp Mol Med, 2025. **57**(7): p. 1482-1491.
2. Luo, J., et al., *Persistent accumulation of therapy-induced senescent cells: an obstacle to long-term cancer treatment efficacy.* Int J Oral Sci, 2025. **17**(1): p. 59.
3. Mongiardi, M.P., et al., *Cancer Response to Therapy-Induced Senescence: A Matter of Dose and Timing.* Cancers (Basel), 2021. **13**(3).
4. Carpenter, V., et al., *Androgen-deprivation induced senescence in prostate cancer cells is permissive for the development of castration-resistance but susceptible to senolytic therapy.* Biochemical Pharmacology, 2021. **193**: p. 114765.
5. Fleury, H., et al., *Exploiting interconnected synthetic lethal interactions between PARP inhibition and cancer cell reversible senescence.* Nat Commun, 2019. **10**(1): p. 2556.
6. Yu, L., et al., *Senescence-Inducing Therapy Sequential NIR-II Mild Photothermal/Senolytic Therapy of Triple Negative Breast Cancer.* Adv Sci (Weinh), 2025. **12**(42): p. e07248.
7. Coppé, J.P., et al., *The senescence-associated secretory phenotype: the dark side of tumor suppression.* Annu Rev Pathol, 2010. **5**: p. 99-118.
8. Saliev, T. and P.B. Singh, *Targeting Senescence: A Review of Senolytics and Senomorphics in Anti-Aging Interventions.* Biomolecules, 2025. **15**(6).
9. Lafontaine, J., et al., *Senolytic Targeting of Bcl-2 Anti-Apoptotic Family Increases Cell Death in Irradiated Sarcoma Cells.* Cancers (Basel), 2021. **13**(3).
10. Martel, J., et al., *Emerging use of senolytics and senomorphics against aging and chronic diseases.* Med Res Rev, 2020. **40**(6): p. 2114-2131.
11. Xiao, S., et al., *Cellular senescence: a double-edged sword in cancer therapy.* Front Oncol, 2023. **13**: p. 1189015.
12. Gayle, S.S., et al., *Targeting BCL-xL improves the efficacy of bromodomain and extra-terminal protein inhibitors in triple-*

negative breast cancer by eliciting the death of senescent cells. J Biol Chem, 2019. **294**(3): p. 875-886.
13. Chen, C., et al., *Senescence-associated secretory phenotype in lung cancer: remodeling the tumor microenvironment for metastasis and immune suppression.* Front Oncol, 2025. **15**: p. 1605085.
14. Dong, Z., et al., *Cellular senescence and SASP in tumor progression and therapeutic opportunities.* Mol Cancer, 2024. **23**(1): p. 181.
15. Wang, L., et al., *Senolytic drugs dasatinib and quercetin combined with Carboplatin or Olaparib reduced the peritoneal and adipose tissue metastasis of ovarian cancer.* Biomed Pharmacother, 2024. **174**: p. 116474.
16. Ahmadinejad, F., et al., *Senolytic-Mediated Elimination of Head and Neck Tumor Cells Induced Into Senescence by Cisplatin.* Mol Pharmacol, 2022. **101**(3): p. 168-180.
17. Feng, T., et al., *Cellular senescence in cancer: from mechanism paradoxes to precision therapeutics.* Mol Cancer, 2025. **24**(1): p. 213.
18. Wang, L., L. Lankhorst, and R. Bernards, *Exploiting senescence for the treatment of cancer.* Nature Reviews Cancer, 2022. **22**(6): p. 340-355.
19. Zhu, Y., et al., *New agents that target senescent cells: the flavone, fisetin, and the BCL-X(L) inhibitors, A1331852 and A1155463.* Aging (Albany NY), 2017. **9**(3): p. 955-963.
20. Robbins, P.D., et al., *Senolytic Drugs: Reducing Senescent Cell Viability to Extend Health Span.* Annu Rev Pharmacol Toxicol, 2021. **61**: p. 779-803.
21. Schreiber, A.R., et al., *Potentiating doxorubicin activity through BCL-2 inhibition in p53 wild-type and mutated triple-negative breast cancer.* Front Oncol, 2025. **15**: p. 1549282.
22. Demaria, M., *Senescent cells: New target for an old treatment?* Mol Cell Oncol, 2017. **4**(3): p. e1299666.
23. Wissler Gerdes, E.O., et al., *Strategies for late phase preclinical and early clinical trials of senolytics.* Mech Ageing Dev, 2021. **200**: p. 111591.
24. Sieben, C.J., et al., *Two-Step Senescence-Focused Cancer Therapies.* Trends Cell Biol, 2018. **28**(9): p. 723-737.
25. Page, M.J., et al., *The PRISMA 2020 statement: an updated guideline for reporting systematic reviews.* BMJ, 2021. **372**: p. n71.
26. Hooijmans, C.R., et al., *SYRCLE's risk of bias tool for animal studies.* BMC Medical Research Methodology, 2014. **14**(1): p. 43.

27. Wakita, M., et al., *A BET family protein degrader provokes senolysis by targeting NHEJ and autophagy in senescent cells.* Nature Communications, 2020. **11**(1): p. 1935.
28. Jia, H.J., et al., *Artesunate ameliorates irinotecan-induced intestinal injury by suppressing cellular senescence and significantly enhances anti-tumor activity.* Int Immunopharmacol, 2023. **119**: p. 110205.
29. Xia, J., et al., *Atorvastatin calcium alleviates 5-fluorouracil-induced intestinal damage by inhibiting cellular senescence and significantly enhances its antitumor efficacy.* Int Immunopharmacol, 2023. **121**: p. 110465.
30. Xia, J., et al., *Artesunate alleviates 5-fluorouracil-induced intestinal damage by suppressing cellular senescence and enhances its antitumor activity.* Discov Oncol, 2023. **14**(1): p. 139.
31. Ren, X., et al., *Caulerpin alleviates cyclophosphamide-induced ovarian toxicity by modulating macrophage-associated granulosa cell senescence during breast cancer chemotherapy.* International Immunopharmacology, 2024. **143**: p. 113513.
32. Guo, Z., et al., *Antibody functionalized curcuma-derived extracellular vesicles loaded with doxorubicin overcome therapy-induced senescence and enhance chemotherapy.* J Control Release, 2025. **379**: p. 377-389.
33. Wang, Z., et al., *Rosiglitazone ameliorates senescence and promotes apoptosis in ovarian cancer induced by olaparib.* Cancer Chemother Pharmacol, 2020. **85**(2): p. 273-284.
34. Xu, Q., et al., *The flavonoid procyanidin C1 has senotherapeutic activity and increases lifespan in mice.* Nature Metabolism, 2021. **3**(12): p. 1706-1726.
35. Deng, L., et al., *Blockade of integrin signaling reduces chemotherapy-induced premature senescence in collagen cultured bladder cancer cells.* Precis Clin Med, 2022. **5**(2): p. pbac007.
36. Chaturvedi, P., et al., *Immunotherapeutic HCW9218 augments anti-tumor activity of chemotherapy via NK cell-mediated reduction of therapy-induced senescent cells.* Mol Ther, 2022. **30**(3): p. 1171-1187.
37. Abdelmoaty, A.A.A., et al., *Senolytic effect of triterpenoid complex from Ganoderma lucidum on adriamycin-induced senescent human hepatocellular carcinoma cells model in vitro and in vivo.* Front Pharmacol, 2024. **15**: p. 1422363.
38. Wang, T., et al., *Combination of PARP inhibitor and CDK4/6 inhibitor modulates cGAS/STING-dependent therapy-induced senescence and provides "one-two punch" opportunity with anti-PD-L1 therapy in colorectal cancer.* Cancer Sci, 2023. **114**(11): p. 4184-4201.

39. Shahbandi, A., et al., *BH3 mimetics selectively eliminate chemotherapy-induced senescent cells and improve response in TP53 wild-type breast cancer.* Cell Death & Differentiation, 2020. **27**(11): p. 3097-3116.
40. Whittle, J.R., et al., *Dual Targeting of CDK4/6 and BCL2 Pathways Augments Tumor Response in Estrogen Receptor-Positive Breast Cancer.* Clin Cancer Res, 2020. **26**(15): p. 4120-4134.
41. Galiana, I., et al., *Preclinical antitumor efficacy of senescence-inducing chemotherapy combined with a nanoSenolytic.* Journal of Controlled Release, 2020. **323**: p. 624-634.
42. Saleh, T., et al., *Clearance of therapy-induced senescent tumor cells by the senolytic ABT-263 via interference with BCL-X(L) -BAX interaction.* Mol Oncol, 2020. **14**(10): p. 2504-2519.
43. Wang, X., et al., *Nifuroxazide boosts the anticancer efficacy of palbociclib-induced senescence by dual inhibition of STAT3 and CDK2 in triple-negative breast cancer.* Cell Death Discovery, 2023. **9**(1): p. 355.
44. Estepa-Fernández, A., et al., *Combination of palbociclib with navitoclax based-therapies enhances in vivo antitumoral activity in triple-negative breast cancer.* Pharmacological Research, 2023. **187**: p. 106628.
45. Softah, A., et al., *The Combination of Radiation with PARP Inhibition Enhances Senescence and Sensitivity to the Senolytic, Navitoclax, in Triple Negative Breast Tumor Cells.* Biomedicines, 2023. **11**(11): p. 3066.
46. Almudimeegh, S., et al., *Talazoparib and radiation enhance the senolytic efficacy of venetoclax in therapy-induced senescent triple-negative breast cancer cells.* Saudi Pharmaceutical Journal, 2025. **33**(5): p. 31.
47. Hann, C.L., et al., *Therapeutic efficacy of ABT-737, a selective inhibitor of BCL-2, in small cell lung cancer.* Cancer Res, 2008. **68**(7): p. 2321-8.
48. Tan, N., et al., *Navitoclax enhances the efficacy of taxanes in non-small cell lung cancer models.* Clin Cancer Res, 2011. **17**(6): p. 1394-404.
49. González-Gualda, E., et al., *Galacto-conjugation of Navitoclax as an efficient strategy to increase senolytic specificity and reduce platelet toxicity.* Aging Cell, 2020. **19**(4): p. e13142.
50. Magkouta, S., et al., *Generation of a selective senolytic platform using a micelle-encapsulated Sudan Black B conjugated analog.* Nature Aging, 2025. **5**(1): p. 162-175.
51. Yamamoto, M., et al., *Gemcitabine Cooperates with Everolimus to Inhibit the Growth of and Sensitize Malignant Meningioma Cells to Apoptosis Induced by Navitoclax, an Inhibitor of Anti-Apoptotic BCL-2 Family Proteins.* Cancers, 2022. **14**(7): p. 1706.

52. Troiani, M., et al., *Single-cell transcriptomics identifies Mcl-1 as a target for senolytic therapy in cancer.* Nature Communications, 2022. **13**(1): p. 2177.
53. Carpenter, V., et al., *Androgen deprivation-induced senescence confers sensitivity to a senolytic strategy in prostate cancer.* Biochemical Pharmacology, 2024. **226**: p. 116385.
54. Hu, Q., et al., *Metformin as a senostatic drug enhances the anticancer efficacy of CDK4/6 inhibitor in head and neck squamous cell carcinoma.* Cell Death & Disease, 2020. **11**(10): p. 925.
55. Hoque, M.M., et al., *Senolysis of gemcitabine-induced senescent human pancreatic cancer cells.* Cancer Reports, 2024. **7**(4): p. e2075.
56. Revskij, D., et al., *Effects of triggers of senescence and senolysis in murine pancreatic cancer cells.* Hepatobiliary & Pancreatic Diseases International, 2024. **23**(6): p. 628-637.
57. Kovacovicova, K., et al., *Senolytic Cocktail Dasatinib+Quercetin (D+Q) Does Not Enhance the Efficacy of Senescence-Inducing Chemotherapy in Liver Cancer.* Front Oncol, 2018. **8**: p. 459.
58. Bousset, L. and J. Gil, *Targeting senescence as an anticancer therapy.* Mol Oncol, 2022. **16**(21): p. 3855-3880.
59. Malaquin, N., et al., *DNA Damage- But Not Enzalutamide-Induced Senescence in Prostate Cancer Promotes Senolytic Bcl-xL Inhibitor Sensitivity.* Cells, 2020. **9**(7).
60. Prasanna, P.G., et al., *Therapy-Induced Senescence: Opportunities to Improve Anticancer Therapy.* J Natl Cancer Inst, 2021. **113**(10): p. 1285-1298.
61. Hayflick, L. and P.S. Moorhead, *The serial cultivation of human diploid cell strains.* Experimental Cell Research, 1961. **25**(3): p. 585-621.
62. Demaria, M., et al., *Cellular Senescence Promotes Adverse Effects of Chemotherapy and Cancer Relapse.* Cancer Discov, 2017. **7**(2): p. 165-176.
63. Campisi, J., *Aging, cellular senescence, and cancer.* Annu Rev Physiol, 2013. **75**: p. 685-705.
64. te Poele, R.H., et al., *DNA damage is able to induce senescence in tumor cells in vitro and in vivo.* Cancer Res, 2002. **62**(6): p. 1876-83.
65. Elmore, L.W., et al., *Adriamycin-induced senescence in breast tumor cells involves functional p53 and telomere dysfunction.* J Biol Chem, 2002. **277**(38): p. 35509-15.
66. Wang, X., et al., *Evidence of cisplatin-induced senescent-like growth arrest in nasopharyngeal carcinoma cells.* Cancer Res, 1998. **58**(22): p. 5019-22.

67. Zhu, Y., et al., *The Achilles' heel of senescent cells: from transcriptome to senolytic drugs.* Aging Cell, 2015. **14**(4): p. 644-58.
68. Yosef, R., et al., *Directed elimination of senescent cells by inhibition of BCL-W and BCL-XL.* Nature Communications, 2016. **7**(1): p. 11190.
69. Hamburger, E.C.B., et al., *Targeting breast cancer senescence in 3D models of bone metastasis.* bioRxiv, 2025: p. 2025.06.26.661856.
70. Cherif, H., et al., *Senotherapeutic drugs for human intervertebral disc degeneration and low back pain.* eLife, 2020. **9**: p. e54693.
71. Greenberg, E.F., et al., *Navitoclax safety, tolerability, and effect on biomarkers of senescence and neurodegeneration in aged nonhuman primates.* Heliyon, 2024. **10**(16): p. e36483.
72. Li, C., et al., *Fisetin suppresses ferroptosis through Nrf2 and attenuates intervertebral disc degeneration in rats.* Eur J Pharmacol, 2024. **964**: p. 176298.
73. Xu, M., et al., *Senolytics improve physical function and increase lifespan in old age.* Nat Med, 2018. **24**(8): p. 1246-1256.
74. Hickson, L.J., et al., *Senolytics decrease senescent cells in humans: Preliminary report from a clinical trial of Dasatinib plus Quercetin in individuals with diabetic kidney disease.* eBioMedicine, 2019. **47**: p. 446-456.
75. Nambiar, A., et al., *Senolytics dasatinib and quercetin in idiopathic pulmonary fibrosis: results of a phase I, single-blind, single-center, randomized, placebo-controlled pilot trial on feasibility and tolerability.* EBioMedicine, 2023. **90**: p. 104481.
76. Joly, F., et al., *A phase II study of Navitoclax (ABT-263) as single agent in women heavily pretreated for recurrent epithelial ovarian cancer: The MONAVI - GINECO study.* Gynecol Oncol, 2022. **165**(1): p. 30-39.
77. Pemmaraju, N., et al., *Addition of navitoclax to ruxolitinib for patients with myelofibrosis with progression or suboptimal response.* Blood Neoplasia, 2025. **2**(1): p. 100056.
78. Liu, N., et al., *Immunotherapy and senolytics in head and neck squamous cell carcinoma: phase 2 trial results.* Nature Medicine, 2025. **31**(9): p. 3047-3061.
79. Wei, A.H., et al., *Venetoclax Combined With Low-Dose Cytarabine for Previously Untreated Patients With Acute Myeloid Leukemia: Results From a Phase Ib/II Study.* J Clin Oncol, 2019. **37**(15): p. 1277-1284.

Table Legend:

Figure Legend:

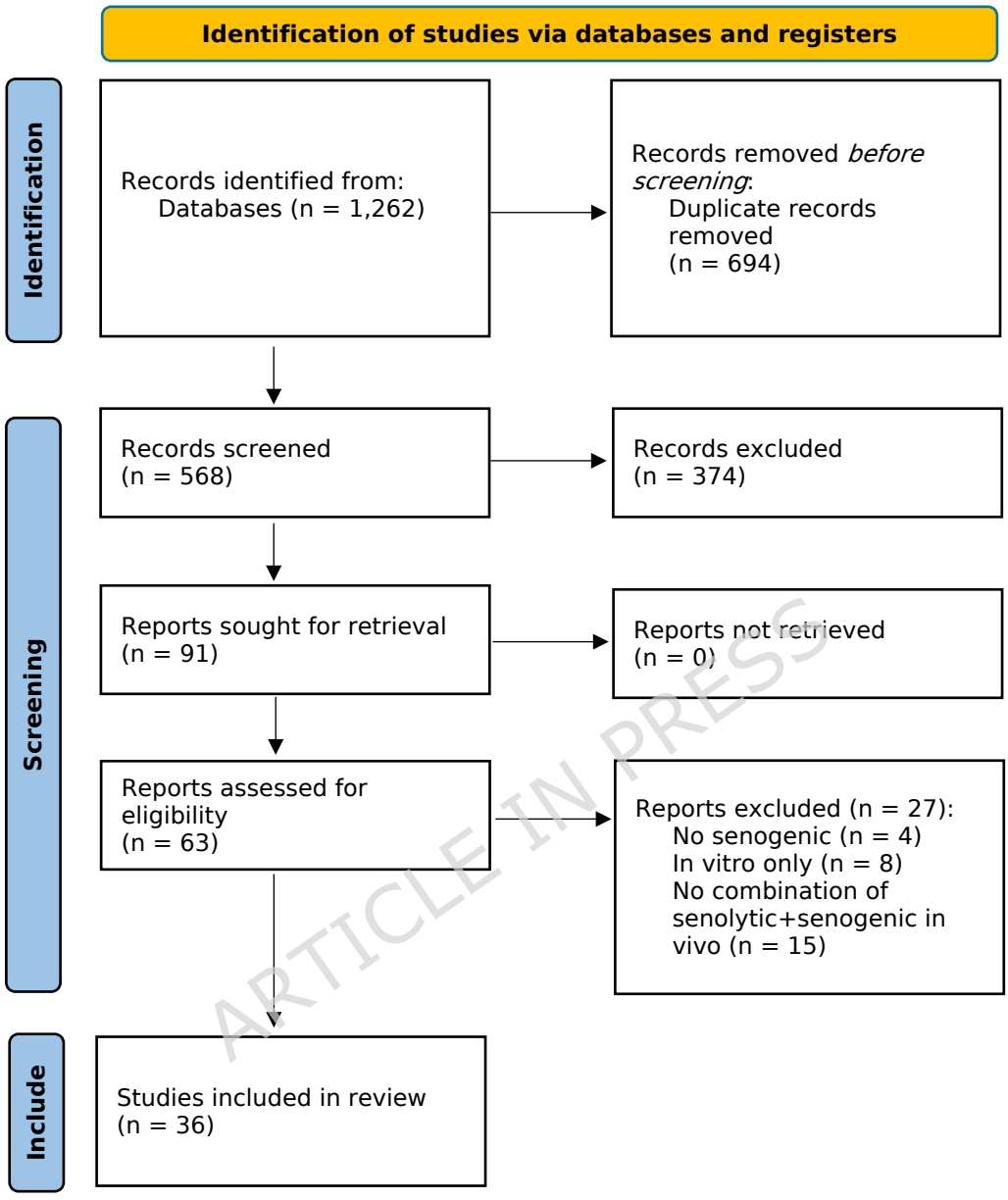

Figure 1. PRISMA 2020 flow diagram.

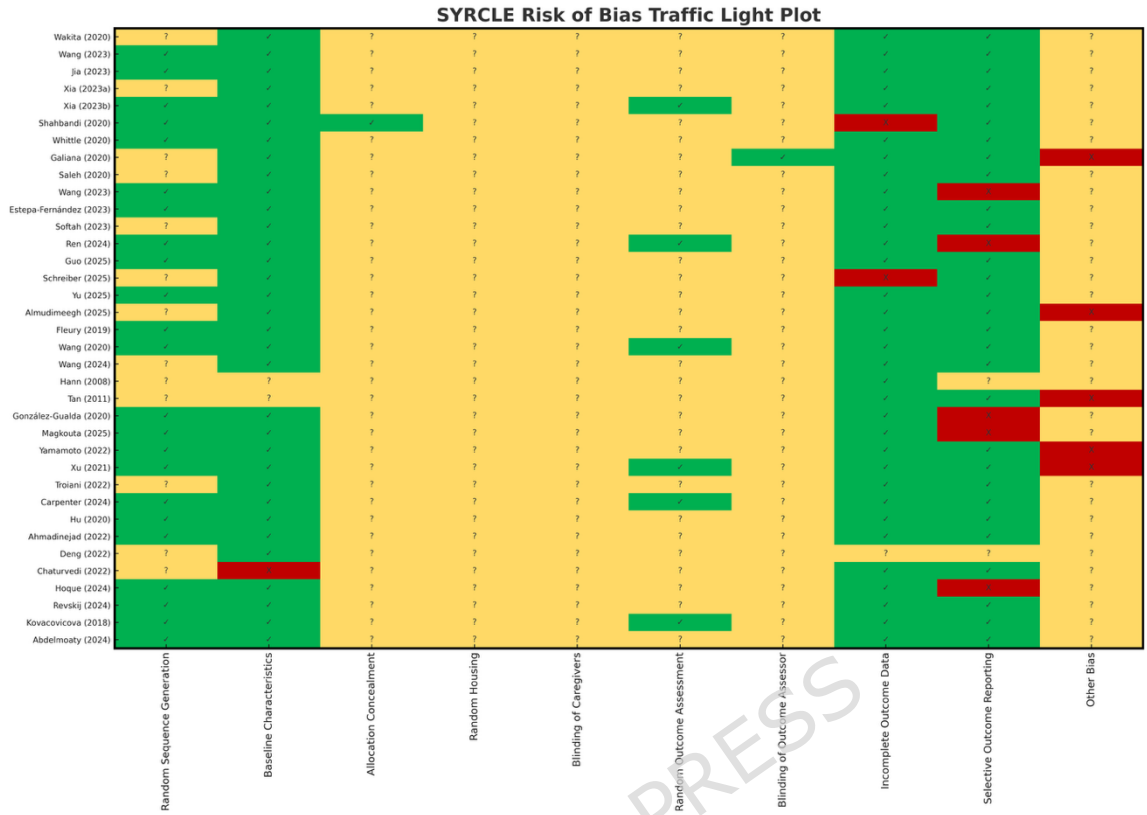

Figure 2. SYRCLE risk of bias traffic light plot for each included study.

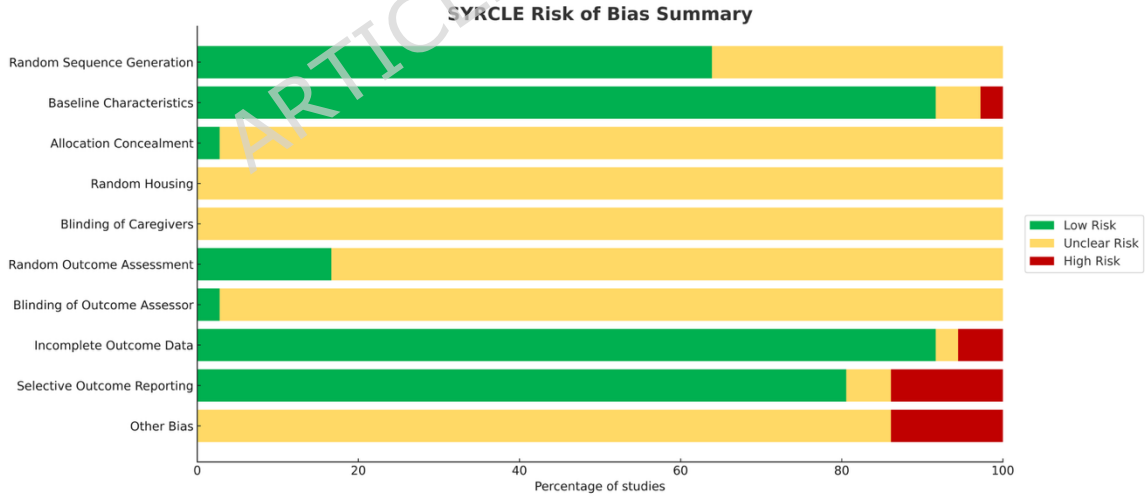

Figure 3. SYRCLE risk of bias summary across domains.

Table 1. Eligibility criteria.

INCLUSION CRITERIA	
Population	Murine cancer models (xenograft, syngeneic, or orthotopic)
Intervention	Senogenic combined with a senolytic or senomorphic agent
Comparison	Senogenic alone
Outcomes	At least one *in vivo* tumor outcome (e.g., volume, weight, survival) and/or mechanistic markers of senescence, SASP cytokines, proliferation, apoptosis, or DNA damage
Study design	Preclinical *in vivo* studies with comparative arms, peer-reviewed publications
EXCLUSION CRITERIA	
Population	Non-cancer or *in vitro* only
Intervention	Immunotherapy or radiation-only arms, no senolytic/senomorphic
Comparison	No comparator arm
Outcomes	Outcomes not reported or incomplete
Study design	Reviews, editorials, conference abstracts, or non-comparative studies

Table 2. Study characteristics of included studies.

Cancer Type	Author (Year)	Journal	Country	Cell Line(s)	Model / Implantation	Group Size	Timepoint
Colorectal cancer	Wakita (2020)	Nat Commun	Japan	HCT116 (1×10^6)	Nude mice; s.c.	n = 4–5	Treat 1 wk post-implant; terminated 6 wks
	Wang (2023)	Cancer Sci	China	CT26 (1×10^6)	BALB/c; injected into right flank	n = 5	Treat when tumor 100 mm^3; endpoint: 50d post treat
	Jia (2023)	Int Immunopharmacol	China	HCT116 (5×10^6)	BALB/c nude; s.c., left flank	n = 6	Tumor reached 1000 mm^3; treat d0–15
	Xia (2023a)	Discov Oncol	China	HCT116 (1×10^7)	BALB/c nude, male; s.c. thigh	n = 6	Treat d14, after ~100 mm^3
	Xia (2023b)	Int Immunopharmacol	China	HCT116 (5×10^6)	BALB/c nude; s.c. axillary	n = 6	Treat when tumor 100 mm^3 → endpoint 1200 mm^3
Breast cancer	Shahbandi (2020)	Cell Death & Differentiation	USA	MMTV-Wnt1 (spontaneous mammary tumor fragments; three independent donor tumors)	C57BL/6j, female; orthotopic mammary fat pad	n = 4-5	Treat when tumor 300mm^3
	Whittle (2020)	Clin Cancer Res	Australia	PDX315, PDX1232, PDX1105 ($1.5–2\times10^5$)	NSG female (PDX); injected into cleared mammary fat pads	NR	Treat when 80–120 mm^3; endpoint: tumor volume exceeded 600 mm^3
	Galiana (2020)	J Control Release	Spain	4T1 (5×10^5)	BALB/cByJ, female; orthotopic mammary fat pad	n = 3-5	Treat 3 days post-implant; endpoint: d21
	Saleh (2020)	Mol Oncology	USA	MDA-MB-231 (2.5×10^6) (breast); A549 (2.5×10^6) (lung)	MDA-MB-231: NSG, female; orthotopic mammary fat pads. A549: NSG, male; s.c. rear flanks	n = 4-14	Treat when tumor ~100 mm^3; endpoint d18 (breast), d20 (lung)
	Wang (2023)	Cell Death Discov	China	4T1 (5×10^5)	BALB/c, female; injected into mammary gland 3 fat pad armpit	n = 6	Treat when 100 mm^3; endpoint: 3 wks post treat
	Estepa-Fernández (2023)	Pharmacol Res	Spain	MDA-MB-231 (2×10^6)	BALB/c nude, s.c. mammary pads	n = 5	Treat when tumor 60 mm^3; endpoint d30

Cancer Type	Author (Year)	Journal	Country	Cell Line(s)	Model / Implantation	Group Size	Timepoint
	Softah (2023)	Biomedicines	Saudi Arabia	4T1 (1×10^6): with or without exposure to 6Gy radiation + 1μM TLZ 72h	BALB/c, female; s.c. rear flanks	n = 6	Treat when tumor 150–200 mm^3, d4; endpoint d14
	Ren (2024)	Int Immunopharmacol	China	MDA-MB-231 (NR)	BALB/c nude, female; orthotopic mammary fat pad	n = 20	Sacrifice when tumor 10% body wt
	Guo (2025)	J Control Release	China	MCF-7 (5×10^5)	BALB/c nude, female; s.c. armpit	n = 4	Treat when tumor 50 mm^3
	Schreiber (2025)	Front Oncol	USA	MDA-MB-231 (5×10^6)	Athymic nude; s.c. bilateral flanks	NR	Treat when 50–100 mm^3; max 2000 mm^3
	Yu (2025)	Adv Sci	China	4T1 (1×10^6)	Nude mice, female; s.c. back	n = 5	Treat when 100 mm^3; endpoint: d24; tumor burden must not exceed 10% body weight
	Almudimeegh (2025)	Saudi Pharmaceutical J	Saudi Arabia	4T1 (1×10^6): with or without exposure to 6Gy radiation + 1μM TLZ 72h	BALB/c, female; s.c. rear flanks	n = 6	Treat when 150–200 mm^3; endpoint d14
Ovarian cancer	Fleury (2019)	Nat Commun	Canada	OV4453, OV1946 (7.5×10^6) (ovarian); MDA-MB-231 (5×10^6) (breast)	NRG, female; injected in right and left flanks	n = 7-16	Treat when tumor 400–500 mm^3; endpoint 800–1000 mm^3 or d14
	Wang (2020)	Cancer Chemother Pharmacol	China	A2780, SKOV3 ($\sim5\times10^6$)	Nude mice; s.c., bilateral flanks	n = 6	A2780: d20; SKOV3: d21
	Wang (2024)	Biomed Pharmacother	China	ID8-luc (2×10^6)	C57BL/6; i.p.	NR	Endpoint: 4 wks
Lung cancer	Hann (2008)	Cancer Res	USA	LX22, LX36 (1×10^6)	C.B-17/SCID; s.c.	NR	Treat when ≥130 mm^3; endpoint d21
	Tan (2011)	Clin Cancer Res	USA	SW1573, A549 and NCI-H1650 (NR)	Athymic nude mice, female; s.c., hind flank	n = 10-15	Treat when tumor 250–350 mm^3
	González-Gualda (2020)	Aging Cell	UK, Spain	A549 (4×10^6), L1475luc (3×10^5)	SCID (CB17-PrkdcSCID/J), female; s.c. flanks (A549); C57BL/6J; tail-vein injection (L1475luc)	n ≈ 10 (A549); n = 4-6 (L1475luc)	Treat when tumor 100 mm^3; endpoint post 3 wks of treatment
Melanoma	Magkouta (2025)	Nat Aging	Greece, UK	B16 (5×10^5)	C57BL/6, male and female; s.c. right flank	n = 4-8	Once tumors became palpable (8–9d post inoculation); endpoint

Cancer Type	Author (Year)	Journal	Country	Cell Line(s)	Model / Implantation	Group Size	Timepoint
							tumor volume <2×10³ or distress
Meningioma	Yamamoto (2022)	Cancers	Japan	IOMM-Lee (1×10⁶)	BALB/cAJcl-nu/nu, male; s.c. bilateral flank regions	n = 8	Treat when tumor >100 mm³; endpoint d36
Prostate cancer	Xu (2021)	Nat Metab	China	PC3 + PSC27 (1.25×10⁶; 1:4)	NOD/SCID; s.c. hind flank	n = 10	Endpoint: bulky disease ≥2000 mm³; ~d56
	Troiani (2022)	Nat Commun	Switzerland	PC3 Luc-shTIMP1	NRG, male; s.c.	n = 5	Treat when 100 mm³; endpoint d42
	Carpenter (2024)	Biomed Pharmacother	USA	MycCaP (1×10⁶)	FVB/N, male; s.c. both flanks	n = 6-8	Treat when tumor ~150 mm³; endpoint tumor burden ≥2 cm³
Head & Neck cancer	Hu (2020)	Cell Death & Disease	China	HSC6 (5×10⁶), PDX (0.8–1.5 mm)	Nude mice; s.c. right armpit (HSC6); s.c. flanks (PDX)	n = 8	Treat when ~100 mm³; 3 wks post treat
	Ahmadinejad (2022)	Mol Pharmacol	USA	OSCC-602 (derived 4NQO lesions, 1×10⁶)	C57BL/6; s.c. rear flank	n = 6	Endpoint: d140
Bladder cancer	Deng (2022)	Precis Clin Med	China	T24 (5×10⁶)	Nude mice; s.c.	n = 6	Treat at d20
Pancreatic cancer	Chaturvedi (2022)	Mol Ther	USA	SW1990 (2×10⁶)	B6 SCID; s.c.	n = 9	Endpoint: d38
	Hoque (2024)	Cancer Reports	Japan	AsPC-1 (2×10⁶)	BALB nude mice, female; s.c. right flank	n = 5	Treat d7; endpoint d21
	Revskij (2024)	Hepato & Pancreatic Diseases Int	Germany	Panc02 (2.5×10⁵)	C57BL/6J, male; injected into pancreatic head	n = 8-9	Treat started d9 post-injection; endpoint d26
Hepatocellular carcinoma	Kovacovicova (2018)	Front Oncol	Estonia	eqFP650-Huh-7 (5×10⁶)	Athymic nude (nu/nu), immunodeficient mice; s.c.	n = 11	Endpoint d23
	Abdelmoaty (2024)	Front Pharmacol	China	HepG2 (~20 mm³)	BALB/c nude; trocar, right flank	n = 8	Treat when tumor 100 mm³

Footnote, Abbreviations: NR = not reported; treat = treatment; wk = week; d = day; mm³ = cubic millimeters; wt = weight; s.c. = subcutaneous; i.p. = intraperitoneal; orthotopic = implantation into the original organ site; trocar = trocar-assisted transplantation; PDX = patient derived xenograft; luc = luciferase-expressing; Gy = gray radiation dose.

Table 3. Senogenic and senolytic/senomorphic interventions used in included studies.

Cancer Type	Author (Year)	Senogenic(s)	Senolytic(s)	Route	Dose of Senogenic(s) (mg/kg)	Dose of Senolytic(s) (mg/kg)
Colorectal cancer	Wakita (2020)	DOX	ARV825	i.p.	1	5
	Wang (2023)	TLZ, Palbo	α-PD-L1	oral (TLZ), oral (Palbo), i.p. (α-PD-L1)	0.33 (TLZ), 20 (Palbo)	200μg
	Jia (2023)	I	Arte	NR	75	30
	Xia (2023a)	5-FU	Arte	i.p.	30	30
	Xia (2023b)	5-FU, Leu	Ator	i.p.	30 (5-FU), 4 (Leu)	30
Breast cancer	Shahbandi (2020)	DOX	ABT-263	i.p. (DOX), oral (ABT-263)	4	50
	Whittle (2020)	Ful, Palbo	Ven	i.p. (Ful), oral (Plabo), oral (Ven)	5 (Ful), 100 (Palbo)	100
	Galiana (2020)	Palbo	GALNP(Nav)	oral (Palbo), i.p. (GALNP(Nav))	50–100	2.5
	Saleh (2020)	DOX (breast) or Eto (lung)	ABT-263	i.p. (DOX or Eto), oral (ABT-263)	2.5 (DOX) or 15 (Eto)	50
	Wang (2023)	Palbo	Nif	oral (Palbo), i.p. (Nif)	50	25 or 50
	Estepa-Fernández (2023)	Palbo	Nav or NavGal	oral (Palbo), oral (Nav), i.p. (NavGal)	50	25 (Nav) or 33.5 (NavGal)
	Softah (2023)	Rad + TLZ	ABT-263	oral (ABT-263)	6Gy Rad and 1μM TLZ	50
	Ren (2024)	CTX	Caulerpin	i.p.	50	4
	Guo (2025)	DOX	CRV ± DR5	i.v.	2	NR
	Schreiber (2025)	DOX	V	i.p. (DOX), oral (V)	1.5	50
	Yu (2025)	Palbo (S), IR1061 (IR), NIR-II laser (L)	IQ Nps (Quercetin + IR1061) or free Quercetin (Qu)	oral (Palbo); tail-vein injection (IQ NPs); external (NIR-II laser)	100 (Palbo); IR1061 10μg; NIR-II laser 1060 nm, 1.0 W cm−2, 10 min	Que: NR; IQ drug loading ~20–25%; IR1061 10μg
	Almudimeegh (2025)	Rad + TLZ	Ven	oral (Ven)	6Gy Rad and 1μM TLZ	100
Ovarian cancer	Fleury (2019)	Ola	ABT-263	i.p. (Ola), oral (ABT-263)	50	50
	Wang (2020)	Ola	Rosi	i.p.	10	10
	Wang (2024)	Carbo or Ola	D + Q	i.p.	2 (Carbo) or 50 (Ola)	5 (D), 50 (Q)
Lung cancer	Hann (2008)	Eto	ABT-737	i.p.	12	100

Cancer Type	Author (Year)	Senogenic(s)	Senolytic(s)	Route	Dose of Senogenic(s) (mg/kg)	Dose of Senolytic(s) (mg/kg)
	Tan (2011)	DTX	Nav	i.v. (DTX), oral (Nav)	7.5	100
	González-Gualda (2020)	Cis	Nav or NavGal	i.p. (Cis), oral (Nav), i.p. (NavGal)	A549: 1.5, L1475: 1	100 (Nav), 85 (NavGal)
Melanoma	Magkouta (2025)	Palbo	mGL392, D, or Q	oral (Palbo), oral (Q), i.p. (mGL392), i.p. (D)	2.5	0.015 (mGL392), 0.125 (D), 1.25 (Q)
Meningioma	Yamamoto (2022)	EVE + GEM	ABT-263	oral (EVE), i.p. (GEM), oral (ABT-263)	2 (EVE), 10 (GEM)	100
Prostate cancer	Xu (2021)	MIT	PCC1	i.p.	0.2	20
	Troiani (2022)	DTX	ABT-263 or S63845	i.p. (DTX), oral (ABT-263), oral (S63845)	10	50 (ABT-263), 25 (S63845)
	Carpenter (2024)	Castration	ABT-263	surgical removal of both testes, oral (ABT-263)	N/A	80
Head & Neck cancer	Hu (2020)	LY2835219	Met	oral (LY2835219), i.p. (Met)	HSC6: 25; PDX: 40	HSC6: 100; PDX: 200
	Ahmadinejad (2022)	Cis	ABT-263	i.p. (Cis), oral (ABT-263)	5	80
Bladder cancer	Deng (2022)	MMC	TFA	i.v. (tail vein)	5	2.5
Pancreatic cancer	Chaturvedi (2022)	G, A	HCW9218	i.p. (G+A), s.c. (HCW9218)	40 (G), 50 (A)	3
	Hoque (2024)	GEM	ABT-737	i.p.	50	35
	Revskij (2024)	Eto	ABT-263	i.p. (Eto), oral (ABT-263)	7	60
Hepatocellular carcinoma	Kovacovicova (2018)	DOX	D+Q	i.p. (DOX), oral (D+Q)	4	5 (D), 50 (Q)
	Abdelmoaty (2024)	DOX	TC	i.p.	6	100 or 250

Footnote, Abbreviations: *DOX = Doxorubicin; ARV825 = BET degrader; I = Irinotecan; Arte = Artesunate; 5-FU = 5-Flourouracil; Leu = Leucovorin; Ator = Atorvastatin calcium; TLZ = Talazoparib; Palbo = Palbociclib; Ful = Fulvestrant; GALNP(Nav) = galactose-targeted Navitoclax nanoparticle; Nif = Nifuroxazide; NavGal = galactose-modified Navitoclax; Rad = radiation; CTX = Cyclophosphamide; Caulerpin = algal metabolite; CRV = Curcuma-derived extracellular vesicles; DR5 = Death Receptor 5 agonist; V, Ven = Venetoclax; Ola = Olaparib; Rosi = Rosiglitazone; Carbo = Carboplatin; D = Dasatinib; Q = Quercetin; mGL392 = small-molecule senolytic; EVE = Everolimus; MIT = Mitoxantrone; PCC1 = Procyanidin C1; Eto = Etoposide; DTX = Docetaxel; Cis = Cisplatin; ABT-263, Nav = Navitoclax; ABT-737 = Bcl-2 family inhibitor; MMC = Mitomycin C; TFA = Integrin α2β1 ligand peptide; G, GEM = Gemcitabine; A = nab-Paclitaxel (Abraxane); HCW9218 = immune senomodulator; TC = Ganoderma lucidum triterpenoid complex; IQ NPs = Quercetin + IR1061 nanoparticles; IR1061 = NIR-II fluorophore.* ***Routes:*** *i.p. = intraperitoneal; i.v. = intravenous; s.c. = subcutaneous; oral = oral gavage; tail-vein = intravenous metastatic delivery; external (laser) = NIR-II laser exposure.*

Table 4. Tumor burden and survival outcomes of included studies.

Cancer Type	Author (Year)	Tumor Volume (mm^3)				Tumor Weight (g)	Survival Outcome
		Control	Senogenic	Senolytic	Combo		
Colorectal Cancer	Wakita (2020)	~1800	~1000	~1200	~600	NR	NR
	Wang (2023)	~1750	TLZ ~1400; Palbo ~1600; TLZ+Palbo ~1200	~1600	TLZ+α-PD-L1 and Palbo+α-PD-L1 ~750, TLZ+Palbo+α-PD-L1 ~50	NR	% Survival: control d45 20%, TLZ d45 40%, TLZ+α-PD-L1 d45 60%, TLZ+Palbo+α-PD-L1 d45 100%, Palbo d32 20%, Palbo+α-PD-L1 d40 40%, TLZ+Palbo d37 40%
	Jia (2023)	~1250	~600	~950	~250	Control ~2.5; Chemo ~1.6; Seno ~2.1; Combo ~0.2	NR
	Xia (2023a)	~1300	~680	~1300	~460	Control ~2.3; Chemo ~1.9; Seno ~2.0; Combo ~0.7	NR
	Xia (2023b)	~1300	(5-FU+Leu) ~700	~1000	~100	Control ~2.0; Senogenic ~1.7; Senolytic ~2.0; Combo ~0.3	NR
Breast cancer	Shahbandi (2020)	Transplant 1 and T2: ~1100, T3: ~600-1100	Transplant 1: ~750, T2: ~700, T3: ~600	Transplant 1: ~900, T2: ~800, T3: NR	Transplant 1: ~500, T2: ~300, T3: ~450-500	NR	Transplant 1: DOX d20, Combo d24; T2: DOX d11, Combo d21; T3: DOX d16, Combo d36

Whittle (2020)	PDX315: ~600; PDX1232 and PDX1105 ~700	Ful: PDX315 ~600, PDX1232 and PDX1105 ~700; Ful+Palbo: PDX315 and PDX1232 ~600, PDX1105 ~700	NR	Ful+Ven: PDX315 and PDX1232 ~600, PDX1105 ~700; Ful+Ven+Palbo: PDX315 ~400, PDX1232 ~600, PDX1105 ~700	NR	PDX315: control ~d20, Ful ~d30,Ful+Ven ~d70, Ful+Palbo ~d120, Ful+Ven+Palbo ~160; PDX1232: control ~d15, Ful ~d22, Ful+Ven ~d39, Ful+Palbo ~d25, Ful+Ven+Palbo ~d100; PDX1105: control ~d12, Ful ~d14, Ful+Ven ~d14, Ful+Palbo ~d14, Ful+Ven+Palbo ~d26
Galiana (2020)	NR	~150	NR	~100	NR	Control d15; Palbo and Combo reported till d18
Saleh (2020)	breast: ~410; lung: ~800	breast: ~170; lung: ~370	breast: ~390; lung: ~800	breast: ~90; lung: ~120	NR	NR
Wang (2023)	~1650	~1300	25Nif: NR; 50Nif: ~1450	Palbo+25Nif: ~1100, Palbo+50Nif: ~900	Control ~1.8, Palbo ~1.4, 25Nif ~1.5, 50Nif NR, Palbo+25Nif ~1.3, Palbo+50Nif ~1.0	NR
Estepa-Fernández (2023)	~190	~90	Nav: ~130; NavGal: NR	Palbo+Nav: ~60; Palbo+NavGal: ~60	NR	NR
Softah (2023)	in % relative to d4: ~500	in % relative to d4: ~350	in % relative to d4: ~350	in % relative to d4: ~50	NR	NR
Ren (2024)	699.7 ± 5.7	234.1 ± 25	441.6 ± 23	366.5 ± 18.1	Reduced qualitatively with senogenic; regardless of added senolytic	NR
Guo (2025)	~1700	(DOX) ~700	(CNV-DOX) ~600	(DR5-CNV-DOX) ~100	Control ~0.8; Senogenic ~0.5; Senolytic (CNV-DOX) ~0.3; Combo ~0.08	NR
Schreiber (2025)	~380	~300	~450	~160	NR	NR

	Yu (2025)	1016	S: 895.6; S+IR: ~600; S+IR+L: 154.6	NR	S+Qu (free drug control): 812.7; S+IQ: ~490; IQ+L: 444.9; S+IQ+L: 23.7	NR	NR
	Almudimeegh (2025)	in % relative to d0: ~500	in % relative to d0: ~450	in % relative to d0: ~300	in % relative to d0: ~100	NR	NR
Ovarian Cancer	Fleury (2019)	In ratio to d0: OV4453: ~2.4; OV1946: ~1.9; MDA-MB-231: ~9	In ratio to d0: OV4453: ~1.6; OV1946: ~1.6; MDA-MB-231: ~4	In ratio to d0: OV4453: ~1.5; OV1946: ~1.9; MDA-MB-231: ~7.5	In ratio to d0: OV4453: ~1.2; OV1946: ~1.3; MDA-MB-231: ~3	NR	NR
	Wang (2020)	A2780: ~1500 SKOV3: ~590	A2780: ~850 SKOV3: ~380	A2780: ~950 SKOV3: ~500	A2780: ~400 SKOV3: ~175	NR	NR
	Wang (2024)	IVIS luminescence: ~7.5×10^6	(C) ~4.5×10^6, (O) ~4.0×10^6	NR	(C+D+Q) ~2.5×10^6, (O+D+Q) ~2.0×10^6	NR	NR
Lung cancer	Hann (2008)	LX22: ~ 1900 LX36: ~ 2100	LX22: ~1000 LX36: ~1900	LX22: ~1900 LX36: ~2000	LX22: ~500 LX36: ~800	NR	NR
	Tan (2011)	SW1573: ~3800; A549: ~1100; NCI-H1650: ~900	SW1573: ~1000; A549: ~700; NCI-H1650: ~600	SW1573: daily ~2400, intermittent ~2300; A549: daily ~850, intermittent ~100; NCI-H1650: daily and intermittent ~700	SW1573: daily and intermittent ~250; A549: daily ~300, intermittent ~400; NCI-H1650: daily and intermittent ~300	NR	NR
	González-Gualda (2020)	A549: ~600	A549: ~350	A549: Nav and NavGal ~ 500	A549: Cis+Nav and Cis+NavGal ~210	NR	NR

Melanoma	Magkouta (2025)	~850	~600	NR	Palbo+D and Palbo+D+Q ~450, Palbo+mGL392 and Palbo+mGL392+Q ~150	NR	NR
Meningioma	Yamamoto (2022)	NR	~220	NR	~110	NR	NR
Prostate Cancer	Xu (2021)	NR	44% reduction vs control	NR	55.2% reduction vs chemo	NR	Combo (MIT+PCC1): 137 vs Senogenic 92.5 d (48.1% longer); Control 70.5 d; Senolytic 77 d
	Troiani (2022)	~900	~420	ABT-263 ~1250; S63845 ~ 1100	DTX+ABT-263 ~300; DTX+S63845 ~250	NR	NR
	Carpenter (2024)	Steady exponential growth	Strong regression, regrowth by d40	No significant suppression	Delayed growth (~+14days)	NR	Control 38d; Castration 56d; ABT-263 36d; Combo 70.5d (+14.5d survival benefit)
Head & Neck Cancer	Hu (2020)	HSC6: ~350; PDX: ~1000	HSC6: ~300; PDX: ~800	HSC6: ~300; PDX: ~800	HSC6: ~100; PDX: ~490	HSC6: control ~0.2, senogenic ~0.115, senolytic ~0.18, combo ~0.050; PDX: control ~0.7, senogenic ~0.4, senolytic ~0.4, combo ~0.2	NR
	Ahmadinejad (2022)	~2200	~1900	~1950	~1700	NR	Combo (Cis+ABT-263): 130 vs Chemo 75 d (57.7% longer)
Bladder Cancer	Deng (2022)	~2200	~1200	~1700	~700	NR	Control ~63 d; Senogenic ~69 d; Senolytic ~66 d; Combo ~75 d
Pancreatic Cancer	Chaturvedi (2022)	~2800	~2100	~2100	~1100	NR	Control ~58 d; Senogenic ~73 d; Senolytic ~65 d; Combo ~76 d
	Hoque (2024)	~350	~240	~250	~190	NR	NR

	Revskij (2024)	NR	NR	NR	NR	Control ~0.20; Senogenic ~0.11; Senolytic ~0.22; Combo ~0.115	NR
Hepatocellular carcinoma	Kovacovicova (2018)	~600	~410	~900	~390	Control ~0.55; Senogenic ~0.35; D+Q ~ 0.75; Combo ~ 0.40	NR
	Abdelmoaty (2024)	~1800	~700	~1400	~400	Control ~2.8; Senogenic ~1.3; Senolytic ~1.8; Combo ~0.5	NR

Footnote, Abbreviations: *NR = not reported; Combo = senogenic + senolytic; d = days; 5-FU+Leu = 5-Flaurauracil plus Leucovorin; DOX = Doxorubicin; Palbo = Palbociclib; TLZ = Talazoparib; α-PD-L1 = anti-PD-L1 antibody; Nif = Nifuroxazide; ABT-263, Nav = Navitoclax; NavGal = galacto-navitoclax; CNV = curcuma derived extracellular vesicles; DR5 = death receptor 5; mGL392 = small-molecule senolytic; C = Carboplatin, O = Olaparib; D = Dasatinib; Q = Quercetin; MIT = Mitoxantrone; PCC1 = Procyanidin C1; Cis = Cisplatin; S63845 = MCL-1 inhibitor; DTX = Docetaxel; A2780, SKOV3 = ovarian cell lines; MDA-MB-231 = breast cancer cell line; PDX = patient-derived xenograft; OV4453, OV1946 = ovarian PDX lines; HSC6 = head and neck cancer line; A549, SW1573, NCI-H1650, LX22, LX36 = lung cancer models.*

Table 5. Senescence, SASP, proliferation and apoptotic/DNA damage markers.

Cancer Type, Author (Year)	**Senescence**				**SASP**					**Proliferation**		**Apoptosis/DNA damage**			
	SA-β-gal	p21	p53	p16	IL-6	IL-1α	IL-1β	TNF-α	IFN-γ	Ki-67	PCNA	Caspase-3	γ-H2AX	BCL2	TUNI
Colorectal Cancer															
Wakita (2020)	NR	↓	NR	NR	NR	NR	NR	NR	NR	NR	NR	↑	↑	NR	NR
Wang (2023)	↓	NR	NR	NR	NR	NR	NR	NR	NR	NR	NR	NR	NR	NR	NR
Jia (2023)	↓	↓	↓	↓	↓	NR	↓	↓	NR	↓	↓	↑	NR	↓	NR
Xia (2023a)	↓	↓	↓	NR	↓	NR	↓	↓	NR	↓	↓	↑	NR	↓	NR
Xia (2023b)	↓	↓	↓	↓	↓	NR	↓	↓	NR	↓	↓	↑	↓	↓	NR
Breast cancer															
Shahbandi (2020)	NR	NR	NR	NR	NR	NR	NR	NR	NR	NR	NR	↑	NR	NR	NR
Whittle (2020)	NR	NR	NR	NR	NR	NR	NR	NR	NR	↓	NR	↑	NR	NR	NR
Galiana (2020)	NR	NR	NR	NR	NR	NR	NR	NR	NR	NR	NR	↑	NR	NR	NR
Saleh (2020)	NR	NR	NR	NR	NR	NR	NR	NR	NR	NR	NR	↑	NR	NR	NR
Wang (2023)	NR	↑	NR	NR	↓	↓	↓	↓	NR	↓	NR	NR	NR	NR	NR
Estepa-Fernández (2023)	NR	NR	↓	NR	NR	NR	NR	NR	NR	NR	NR	NR	NR	NR	↑
Softah (2023)	NR	NR	NR	NR	NR	NR	NR	NR	NR	NR	NR	NR	NR	NR	↑
Ren (2024)	NR	↓	↓	NR	NR	NR	NR	NR	NR	NR	NR	NR	NR	NR	NR
Guo (2025)	NR	NR	NR	↓	↓	NR	NR	NR	↑	NR	NR	NR	NR	NR	NR
Schreiber (2025)	↓	NR	NR	NR	NR	NR	NR	NR	NR	↓	NR	NR	NR	NR	NR
Yu (2025)	NR	NR	NR	NR	NR	NR	NR	NR	NR	↓	NR	NR	NR	NR	NR
Almudimeegh (2025)	NR	NR	NR	NR	NR	NR	NR	NR	NR	NR	NR	NR	NR	NR	↑
Ovarian Cancer															

Fleury (2019)	NR	NR	NR	NR	NR	NR	NR	NR	NR	NR	NR	NR	NR	NR	NR
Wang (2020)	NR	NR	NR	NR	NR	NR	NR	NR	NR	NR	NR	NR	NR	NR	NR
Wang (2024)	↓	NR	NR	NR	NR	NR	NR	NR	NR	NR	NR	NR	NR	NR	NR
Lung cancer															
Hann (2008)	NR	NR	NR	NR	NR	NR	NR	NR	NR	NR	NR	NR	NR	NR	NR
Tan (2011)	NR	NR	NR	NR	NR	NR	NR	NR	NR	NR	NR	NR	NR	NR	NR
González-Gualda (2020)	↓	↓	NR	NR	NR	NR	NR	NR	NR	↓	NR	NR	NR	NR	↑
Melanoma															
Magkouta (2025)	↓	NR	NR	NR	NR	NR	NR	NR	NR	NR	NR	↑	NR	NR	NR
Meningioma															
Yamamoto (2022)	NR	NR	NR	NR	NR	NR	NR	NR	NR	NR	NR	↑	NR	NR	NR
Prostate Cancer															
Xu (2021)	↓	↓	NR	↓	↓	↓	↓	NR	NR	NR	NR	↑	↑	NR	NR
Troiani (2022)	↓	NR	NR	↓	NR	NR	NR	NR	NR	↓	NR	↑	NR	↓	NR
Carpenter (2024)	NR	NR	NR	NR	NR	NR	NR	NR	NR	NR	NR	↑	NR	NR	NR
Head & Neck Cancer															
Hu (2020)	NR	NR	NR	NR	NR	NR	NR	NR	NR	↓	↓	NR	NR	NR	NR
Ahmadinejad (2022)	↓	NR	NR	NR	NR	NR	NR	NR	NR	↓	NR	↑	-	NR	NR
Bladder Cancer															
Deng (2022)	↓	NR	NR	NR	NR	NR	NR	NR	NR	NR	NR	↑	NR	NR	NR
Pancreatic Cancer															
Chaturvedi (2022)	NR	↓	NR	NR	↓	↓	NR	NR	↑	NR	NR	NR	NR	NR	NR

Hoque (2024)	NR	NR	NR	NR	NR	NR	NR	NR	NR	NR	NR	NR	NR	NR	NR
Revskij (2024)	NR	NR	NR	NR	NR	NR	NR	NR	NR	↓	NR	NR	-	NR	NR
Hepatocellular carcinoma															
Kovacovicova (2018)	-	NR	NR	NR	NR	NR	NR	NR	NR	NR	NR	NR	NR	NR	NR
Abdelmoaty (2024)	↓	↓	NR	↓	↓	↓	↓	NR	NR	↓	NR	NR	NR	NR	↑

Footnote, Abbreviations: *↓ = decreased in combination vs senogenic; ↑ = increased in combination vs senogenic; - = no significant change compared to senogenic alone; NR = not reported in the in vivo component; SA-β-gal = senescence-associated β-galactosidase; p21 = cyclin-dependent kinase inhibitor 1A (CDKN1A); p53 = tumor protein p53; p16 = cyclin-dependent kinase inhibitor 2A (CDKN2A); IL-6 = interleukin-6; IL-1α = interleukin-1 alpha; IL-1β = interleukin-1 beta; TNF-α = tumor necrosis factor alpha; IFN-γ = interferon gamma; Ki-67 = proliferation-associated nuclear antigen (MKI67); PCNA = proliferating cell nuclear antigen; Caspase-3 = cysteine-aspartic protease 3; γ-H2AX = phosphorylated histone H2A variant X; BCL2 = B-cell lymphoma 2; TUNEL = terminal deoxynucleotidyl transferase dUTP nick-end labeling.*

Table 6. Toxicity and safety findings.

Cancer Type	Author (Year)	Toxicity Assessment Summary	Body Weight / Organ Health Outcomes	Conclusions on Safety
Colorectal cancer	Wakita (2020)	NR	NR	NR
	Wang (2023)	NR	Stable body weight across all groups.	Body weight stable across all treatment groups, suggesting tolerability of combination treatment.
	Jia (2023)	Combination prevented intestinal aging via p-mTOR inhibition and maintained body weight.	Body weight stable (Ctrl ~25.5 g; Combo ~26.5 g).	Combination improved gastrointestinal tolerance vs senogenic alone.
	Xia (2023a)	Combination reduced diarrhea without disturbing body weight.	Body weight stable (~98–100 % baseline).	Combination improved GI side effects; no toxicity.
	Xia (2023b)	Combination reduced diarrhea and stabilized food/water intake.	Body weight stable (~100 % baseline).	Combination was better tolerated than 5-FU + Leu.
Breast cancer	Shahbandi (2020)	CBC parameters and body weight monitored. No severe drops in blood counts; no significant weight loss.	Body weight remained stable; hematological parameters (RBC, WBC, platelets) remained within normal range. No organ histology reported.	Combination regimen appears well tolerated under study conditions; no evident systemic toxicity.
	Whittle (2020)	Separate toxicity study in healthy BALB/c mice reported stable body weight and transient leukopenia that resolved after a rest period. These findings were not in the PDX efficacy experiment.	NR	NR
	Galiana (2020)	Nav-loaded nanoparticles did not increase Palbo-associated toxicity; combination reduced metastasis without added systemic toxicity.	<10% weight loss in all groups (Palbo ~4%, Combo ~3.5%); platelet counts remained stable; no significant organ damage reported.	No major toxicity reported; some animal loss occurred resulting in variable final group sizes (n = 3-5); platelet counts stable and weight loss <10%.
	Saleh (2020)	NR	NR	NR
	Wang (2023)	No treatment-related weight loss or liver/kidney histopathology reported in xenograft experiments.	Body weight stable across groups; liver and kidney H&E unremarkable (data not shown).	Combination Palbo+Nif was well tolerated; no overt systemic toxicity reported.

	Estepa-Fernández (2023)	Lung metastatic clusters significantly reduced with combination treatments; hematological and biochemical evaluation of treatments showed reduced toxicity with use of NavGal as it is less cytotoxic in non-senescent cells.	Control ~20g; Palbo ~19g; Nav ~20; Palbo+Nav ~17.5g; Palbo+NavGal ~17.5g.	Combination reduced tumor size, maintained body weight, and did not show significant increase in toxicity with use of Palbo+NavGal.
	Softah (2023)	NR	NR	NR
	Ren (2024)	CTX alone caused weight loss and ovarian toxicity; combination restored follicles and AMH/FSHR.	Body weight stable (~20 g vs ~19 g in senogenic).	Caulerpin reduced CTX-induced follicle loss and improved ovarian function.
	Guo (2025)	DR5-targeted Curcuma EVs with DOX showed excellent biosafety and antitumor effect.	Body weight stable (~21 g combo vs ~19.5 g senogenic).	Combination improved biosafety.
	Schreiber (2025)	NR toxicity; body weight stable.	Final weight ~97 % of baseline vs ~101% chemo.	Well tolerated, no evidence of systemic toxicity.
	Yu (2025)	No significant toxicity detected across treatment groups; hemolysis <5%; serum markers within normal range, and organ H&E showed no abnormalities.	Body weight remained stable with no abnormalities in organ condition.	IQ NPs and S+IQ+L were well-tolerated with no evidence of systemic toxicity.
	Almudimeegh (2025)	NR	NR	NR
Ovarian cancer	Fleury (2019)	NR	NR	NR
	Wang (2020)	NR	NR	NR
	Wang (2024)	Luminescence imaging showed no abnormal health indicators.	Body weight stable (~21–23 g) across all groups.	Combination (Carbo/Ola + D + Q) well tolerated; no added toxicity.
Lung cancer	Hann (2008)	NR	NR	NR
	Tan (2011)	Reported as well tolerated with the addition of senolytic.	Body weight stable across all treatment groups.	Combination was well tolerated and did not result in adverse body weight change.
	González-Gualda (2020)	No significant toxicity observed; platelet counts remained within normal ranges across groups.	Body weight remained stable across all treatment groups; no additional organ toxicity assessments were reported.	Treatments were well tolerated with no evidence of weight loss or hematological toxicity.
Melanoma	Magkouta (2025)	No systemic toxicity detected. Serum chemistry levels remained within normal limits, and histological examination of major organs showed no treatment-related abnormalities.	Body weight NR. Histology of liver, kidney, lung and spleen showed no pathological changes.	mGL392 was well-tolerated with no evidence of systemic, hematological or organ-level toxicity.

Meningioma	Yamamoto (2022)	NR	Body weight NR for EVE+GEM vs combo with ABT-263 groups.	NR
Prostate cancer	Xu (2021)	Comprehensive toxicity evaluation: hematology and organ histology normal.	Body weight stable (~22–23 g).	No systemic or hematologic toxicity; organ integrity preserved.
	Troiani (2022)	NR	NR	NR
	Carpenter (2024)	NR	NR	NR
Head & Neck cancer	Hu (2020)	No overt toxicity in liver or kidney pathology.	Stable body weight across all groups.	Well tolerated, no overt toxicity reported.
	Ahmadinejad (2022)	Platelet and neutrophil counts unaffected; no thrombocytopenia or neutropenia from ABT-263.	NR	Combination showed no hematologic toxicity; well tolerated.
Bladder cancer	Deng (2022)	NR	NR	NR
Pancreatic cancer	Chaturvedi (2022)	NR	NR	NR
	Hoque (2024)	NR toxicity: no organ or serum analyses reported.	Body weight remained generally stable: Control ~23, GEM ~22.5, ABT ~19, and Combo ~20.	Mild weight reduction in ABT-737 groups; all mice survived and tolerated treatment.
	Revskij (2024)	NR	NR	NR
Hepatocellular carcinoma (HCC)	Kovacovicova (2018)	NR	NR	NR
	Abdelmoaty (2024)	Triterpenoid complex reduced DOX toxicity, improved inflammation profile. Combination normalized serum ALT, AST and creatinine.	Body weight stable (~26 g combo vs ~19.5 g chemo).	Combination reversed DOX-induced toxicity and improved systemic tolerance.

Footnote, Abbreviations: *NR = not reported; p-mTOR = phosphorylated mammalian target of rapamycin; GI = gastrointestinal; 5-FU = 5-Fluorouracil; Leu = Leucovorin; CTX = Cyclophosphamide; AMH = anti-Müllerian hormone; FSHR = follicle-stimulating hormone receptor; Palbo = Palbociclib; TLZ = Talazoparib; α-PD-L1 = anti-PD-L1 antibody; Nif = Nifuroxazide; EVE = Everolimus; G, GEM = Gemcitabine; ABT-737 = Bcl-2 inhibitor; ABT-263, Nav = Navitoclax; NavGal = galacto-navitoclax; mGL392 = small-molecule senolytic; DR5 = death receptor 5; EVs = extracellular vesicles; DOX = Doxorubicin; Carbo = Carboplatin; Ola = Olaparib; D + Q = Dasatinib + Quercetin; Rosi = Rosiglitazone; PCC1 = Procyanidin C1; ABT-263 = Navitoclax; ALT = alanine aminotransferase; AST = aspartate aminotransferase.*

Table 7. Key results and clinical implications.

Cancer Type	Author (Year)	Clinical Applicability	Key Results	Conclusions
Colorectal Cancer	Wakita (2020)	Proof-of-concept for senolytic co-treatment enhancing chemotherapeutic efficacy in solid tumors.	ARV825 + DOX reduced tumor volume (~600 mm^3 vs ~1000 mm^3), ↓ p21; ↑ caspase-3; ↑ γ-H2AX.	Supports BET-targeting senolytics to suppress senescence and augment chemotherapy.
	Wang (2023)	Dual PARP + CDK4/6 inhibition induces strong therapy-induced senescence and immune activation creating a therapeutic window that synergizes with PD-L1 blockade. Representing a potential one-two punch approach.	Triple treatment markedly ↓ SA-β-gal, tumor growth, ↑ median survival and 60% of mice achieved complete tumor remission.	Triple treatment enhanced anti-tumor durability through senescence induction and PDL-1 mediated clearance of senescent cells, producing superior tumor control and survival. Further longitudinal and translational studies are needed to validate safety, durability, and clinical potential.
	Jia (2023)	Suggests dual chemo-senolytic targeting to reduce tumor burden and prevent intestinal aging.	I + Arte reduced tumor volume (~250 mm^3 vs 600 mm^3), ↓ SA-β-gal, p21, p53, p16, IL-6, IL-1β, TNF-α, Ki-67, PCNA, BCL2; ↑ caspase-3.	Combination therapy enhanced anti-tumor activity and reduced toxicity.
	Xia (2023a)	Demonstrates additive anti-tumor effect via suppression of proliferation and SASP.	5-FU + Arte reduced tumor volume (~460 mm^3 vs 680 mm^3), ↓ SA-β-gal, p21, p53, IL-6, IL-1β, TNF-α, Ki-67, PCNA, BCL2; ↑ caspase-3.	Artesunate enhances 5-FU efficacy through apoptosis induction and SASP suppression.
	Xia (2023b)	Shows multi-agent synergy targeting both senescence and metabolic signaling.	5-FU + Leu + Ator reduced tumor volume (~100 mm^3 vs 700 mm^3), ↓ SA-β-gal, p21, p53, p16, IL-6, IL-1β, TNF-α, Ki-67, PCNA, BCL2; ↑ caspase-3, γ-H2AX.	Statin-based senotherapeutics potentiate chemo efficacy and induce apoptosis.
Breast Cancer	Shahbandi (2020)	Proof-of-concept that clearing chemotherapy-induced senescent cells with a BH3 mimetic (ABT-263) can enhance tumor regression and delay relapse in breast cancer.	Across three independent MMTV-*Wnt*1 transplants, DOX followed by ABT-263 ↓ tumor growth and extended relapse-free survival compared with DOX alone. One transplant showed significant benefit, one showed a strong trend toward improvement, and one showed a directional but non-significant ↓ in tumor growth.	The differing outcomes across the three transplants likely reflect biological variability among individual MMTV-*Wnt*1 tumors, which vary in senescence induction and chemosensitivity. Despite this variability, two transplants demonstrated clear benefit (one significant, one borderline), and the third still showed reduced tumor growth, supporting a consistent overall therapeutic effect of senolytic augmentation.
	Whittle (2020)	Demonstrates a clinically relevant strategy combining senogenic therapy (Ful, Palbo) with senolytic Ven to suppress tumor proliferation in ER+ breast cancer.	The triple combination slowed tumor growth, ↓ Ki-67 while ↑ Caspase-3.	Combination therapy shows potential to enhance short-term antitumor effects, however, in vivo efficacy was moderate, and further studies are required to evaluate tumor regression, durability of response and toxicity within tumor-bearing models.

Galiana (2020)	Demonstrates senolytic nanoparticle delivery to enhance CD4/6-induced senescence therapy while reducing toxicity.	Palbo+GALNP-(Nav) ↓ tumor volume, ↓ lung metastasis, ↑ caspase-3; <10% weight loss; platelet counts preserved	Nanoparticle-encapsulated Navitoclax improved Palbo efficacy and safety
Saleh (2020)	Supports use of BH3-mimetic senolytics to eliminate chemotherapy-induced senescent tumor cells and enhance cytotoxic efficacy in solid tumors.	Nav+DOX (breast) or Nav+Eto (lung) ↓ tumor growth more than chemo alone; ↑ caspase-3, effective across both orthotopic breast and s.c. lung xenografts.	Combining chemotherapy with Navitoclax enhanced senescent-cell clearance and strengthened anti-tumor efficacy in both breast and lung cancer models.
Wang (2023)	Demonstrates a rational senogenic-senomorphic strategy, where adding Nif improved efficacy of CDK4/6 inhibition (Palbo) by suppressing SASP factors of induced senescence.	Combination ↓ tumor growth, lung metastasis, Ki-67, and targeted the SASP (IL6, IL1A, IL1B, TNFA) of induced senescence cells (p21).	The combination suppresses proliferation, tumor growth and metastasis. These findings support its potential for a senogenic-senomorphic strategy. Future studies could test the integration of a senolytic agent to determine whether senescent cell clearance further enhances therapeutic durability.
Estepa-Fernández (2023)	Senolytic-enhanced CDK4/6 therapy offers a potentially safer, more effective treatment strategy.	Combination of Palbo+Nav or Palbo+NavGal ↓ tumor growth and lung metastasis, with NavGal showing ↓ toxicity and stable body weights.	Palbo+NavGal improved antitumor efficacy without added systemic toxicity, supporting its translational potential.
Softah (2023)	Combining DNA-damaging therapy (radiation) with PARP inhibition and senolytic targeting may enhance clearance of therapy-damaged tumor cells.	Radiation therapy + PARPi (TLZ) + Nav ↑ tumor-cell destruction and necrosis (H&E) and showed higher percentages of tumor-cell death and ↓ tumor size compared with single or double treatments.	Triple treatment enhanced anti-tumor efficacy.
Ren (2024)	Illustrates potential fertility-preserving senotherapy with maintained anti-tumor efficacy.	CTX + Caulerpin ↓ p21, p53; restored ovarian AMH/FSHR.	Caulerpin mitigates chemo-toxicity while maintaining tumor control.
Guo (2025)	Introduces senolytic-nanovesicle drug delivery for targeted anti-tumor and SASP suppression.	DR5-Curcuma EV + DOX ↓ tumor volume (~100 mm^3 vs 700 mm^3 chemo), ↓ p16, IL-6; ↑ IFN-γ.	Nanoscale senotherapy exhibits synergistic tumor and SASP suppression with safety.
Schreiber (2025)	Validates apoptotic pathway targeting using clinically available senolytics.	V + DOX ↓ tumor volume (~160 mm^3 vs 300 mm^3), ↓ SA-β-gal, Ki-67.	BCL2-inhibiting senolytics potentiate DOX-induced apoptosis.
Yu (2025)	Demonstrates potential for combining senescence-inducing therapy with nanoparticle-based photothermal senolytic to enhance tumor clearance.	S+IQ+L produced the strongest anti-tumor response, ↓ tumor volume significantly, with stable body weight.	Nanoparticle-delivered senolytics combined with photothermal activation markedly augment Palbo therapy and may represent a promising approach for eliminating therapy-induced senescent tumor cells.

	Almudimeegh (2025)	Demonstrates potential of senescence-priming (TLZ + Rad) to enhance Ven responsiveness, suggesting a feasible therapeutic sequence in reducing tumor burden.	Triple treatment produced the strongest tumor suppression, with the highest tumor cell destruction (43%) on H&E analysis.	Ven effectively limited tumor growth when tumors were preconditioned with senescence-inducing therapy, supporting senolytic augmentation as a strategy to improve treatment outcomes.
Ovarian Cancer	Fleury (2019)	Demonstrates translational potential for using a PARPi to induce senescence followed by a senolytic hit with ABT-263 to reduce tumor burden.	Combination therapy significantly ↓ tumor growth compared with either monotherapy in both ovarian and breast cancer xenograft models.	Dual therapy improved *in vivo* tumor control by eliminating the senescent cell population generated by PARP inhibition, supporting a feasible therapeutic sequence for enhancing PARPi efficacy.
	Wang (2020)	Establishes foundational *in vivo* evidence for senolytic–chemo synergy.	Ola+Rosi reduced tumor volume (A2780: 400 mm^3 vs 850 mm^3).	Combination therapy enhanced anti-tumor activity.
	Wang (2024)	Evaluates combination of clinically relevant senolytics (D+Q) with platinum-based chemo.	Carbo/Ola+D+Q lowered tumor luminescence signal (~2.5–2.0×10^6 vs 4.5×10^6), ↓ SA-β-gal	D+Q synergize with standard chemo to suppress tumor growth.
Lung cancer	Hann (2008)	Conducted in patient-derived xenografts, providing a clinically relevant platform for evaluating chemo-senolytic synergy. Supports combining chemotherapy with a Bcl-2 family inhibitor to enhance tumor control.	Combination therapy reduced tumor growth more than either ABT-737 or etoposide alone in both LX22 and LX36 models.	Co-targeting survival pathways with ABT-737 improves chemotherapeutic response *in vivo.*
	Tan (2011)	Demonstrates potential for combining chemotherapy with Bcl-2 family inhibition to improve tumor control in NSCLC models.	DTX+Nav produced the greatest tumor suppression across SW1573, A549, and NCI-H1650 xenografts, outperforming monotherapy.	Co-targeting apoptotic resistance with Nav enhanced DTX efficacy in vivo, supporting chemo-senolytic combination strategies.
	González-Gualda (2020)	Demonstrates a clinically relevant strategy to enhance Cis response while potentially reducing systemic toxicity with use of NavGal, a senescence-targeted derivative designed to avoid dose-limiting effects associated with Nav alone.	Cis+NavGal produced the strongest anti-tumor effect in A549 xenografts, ↓ tumor volume significantly. In the orthotopic luciferase model Cis+NavGal prevented tumor progression maintaining a ~1-fold luciferase signal versus ~3-4-fold increases in controls and ~1.5-2-fold with Cis alone, while avoiding the platelet-related toxicity commonly associated with Nav.	NavGal selectively targets therapy-induced senescent tumor cells, overcoming the limitations of Nav by delivering senolytic activity with reduced possible systemic toxicity. Combined with Cis, NavGal provides superior tumor control and prevented relapse signals, supporting the therapeutic value of senescence-directed drug design.

Melanoma	Magkouta (2025)	Demonstrates feasibility of using a senolytic targeting (mGL392) to selectively clear therapy-induced senescent melanoma cells and enhance therapeutic response.	mGL392 ↓ GLF16 senescence burden, ↓ SA-β-gal, ↑ caspase-3, ↓ cell viability (MTT), and significantly suppressed tumor growth with combination treatment producing the smallest tumor volumes.	Senolytic addition improved anti-tumor efficacy by eliminating the senescent cell population induced by standard chemotherapy, supporting senescence-targeting as a strategy to augment melanoma treatment.
Meningioma	Yamamoto (2022)	Demonstrates potential for adding Bcl-2 family inhibition treatment to improve tumor control in meningioma models.	Combination of EVE+GEM+ABT-263 showed a significant ↓ in tumor volume as well as ↑ caspase-3.	Combination therapy shows promise as an adjuvant strategy to improve meningioma cancer treatment.
Prostate Cancer	Xu (2021)	Demonstrates senolytic clearance of stromal senescence to augment therapy.	PCC1+MIT → 55 % tumor volume reduction vs chemo alone; ↑ survival (137 d vs 92 d), ↓ SA-β-gal, p21, p16, IL-6, IL-1α, IL-1β; ↑ caspase-3, γ-H2AX.	Natural senolytic compounds can target therapy-induced senescence in TME.
	Troiani (2022)	Demonstrates that senolytic co-treatment with either MCL-1 or BCL-2 inhibitors can enhance chemotherapeutic efficacy by targeting therapy-induced senescence.	Combinations ↓ tumor volume, metastasis, SA-β-gal, p16, BCL2, Ki-67; ↑ caspase-3. (MCL-1 inhibitor S63845 showed the strongest senolysis and metastatic suppression in combination with DTX).	Both senolytics enhance DTX efficacy by clearing senescent tumor cells. MCL-1 inhibition provided superior senolytic and anti-metastatic activity. Longitudinal and survival studies are needed to confirm durability and clinical relevance of these effects.
	Carpenter (2024)	Demonstrates the potential of surgical castration to generate a senescent tumor state that can be selectively targeted with senolytic therapy in prostate cancer.	When castration was followed by ABT-263 treatment, tumor relapse was delayed and overall survival improved (~70.5 combo vs 56 days castration only), although combined anti-tumor effect remained transient.	Sequential senescence induction by surgical castration followed by senolytic therapy provides modest benefit by delaying relapse, supporting the concept of senogenic priming. However, responses were stated to be temporary, indicating that senolytics alone cannot sustain long-term tumor suppression in this model.
Head & Neck Cancer	Hu (2020)	Combination of CDK4/6 inhibitor (LY2835219) + Met as a senomorphic enhanced therapeutic efficacy in the xenograft models.	Combination significantly ↓ tumor volume, tumor weight, ↓ Ki-67 and PCNA.	Demonstrates synergistic short-term antitumor efficacy; requires further evaluation of longevity.
	Ahmadinejad (2022)	First *in vivo* demonstration of ABT-263 + Cis synergy in oral carcinoma.	ABT-263+Cis extended survival (130 d vs 75 d), ↓ SA-β-gal, Ki-67; ↑ caspase-3; γ-H2AX no change; no hematologic toxicity.	BCL2/BCL-xL inhibition enhances apoptosis and mitigates chemo resistance.
Bladder Cancer	Deng (2022)	Explores peptide-based senotherapeutic strategy.	MMC+TFA reduced tumor volume (~700 mm^3 vs 1200 mm^3), ↓ SA-β-gal, ↑ caspase-3 and survival.	Integrin-targeted senotherapy shows potential for bladder malignancies.
Pancreatic Cancer	Chaturvedi (2022)	Evaluates senolytic immune-modulating co-therapy.	G+A+HCW9218 reduced tumor volume (~1100 mm^3 vs 2100 mm^3),	Immuno-senotherapeutic modulation enhances chemo response in PDAC.

			↓ p21, IL-6, IL-1α; ↑ IFN-γ and ↑ survival.	
	Hoque (2024)	Demonstrates potential for combining a senescence-inducing chemotherapeutic with a senolytic agent to enhance tumor control.	GEM+ABT-737 produced the greatest tumor ↓ compared with either monotherapy.	Combination therapy shows promise as an adjuvant strategy to improve pancreatic cancer treatment outcomes.
	Revskij (2024)	Exploratory evidence for senogenic-senolytic co-treatment in orthotopic pancreatic cancer, though in vivo effects remain limited.	Eto alone and in combination with ABT-263 produced comparable ↓ in tumor weight. Only the combination ↓ Ki-67 proliferation, while γ-H2AX induction was similar between Eto and combo group. No tumor volume tracking, survival analysis, or toxicity assessment was reported.	In vivo responses were modest and incomplete, indicating that while senolytic addition may enhance antiproliferative activity, the therapeutic impact remains uncertain in this case. More comprehensive studies including tumor growth kinetics, survival outcomes, and safety evaluation are needed before drawing conclusions about clinical relevance.
Hepatocellular Carcinoma	Kovacovicova (2018)	This study shows that senolytic strategies do not universally enhance chemotherapy efficacy and emphasizes the need to verify senolytic activity in each tumor context before considering clinical translation.	Dox ↓ tumor growth, whereas D+Q alone ↑ tumor burden, and combination did not improve tumor control when compared to Dox alone. The combination also failed to clear Dox-induced senescent cells as indicated by SA-β-gal.	D+Q addition was not an effective senolytic in this HCC model and did not enhance the efficacy of Dox, highlighting that senolytic responses are highly context dependent.
	Abdelmoaty (2024)	Demonstrates senomorphic protection against doxorubicin toxicity.	DOX + TC → tumor ↓ (400 mm^3 vs 700 mm^3), ↓ SA-β-gal, p21, p16, IL-6, IL-1α, IL-1β, Ki-67; body weight restored.	Senomorphic triterpenoids mitigate chemo toxicity and inflammation while retaining efficacy.

Footnote, Abbreviations: *↓ = decreased; ↑ = increased; SA-β-gal = senescence-associated β-galactosidase; p21 = cyclin-dependent kinase inhibitor 1A; p53 = tumor suppressor protein 53; p16 = cyclin-dependent kinase inhibitor 2A; IL = interleukin; TNF-α = tumor necrosis factor-alpha; IFN-γ = interferon-gamma; Ki-67 = proliferation marker; PCNA = proliferating cell nuclear antigen; Caspase-3 = cysteine-aspartic protease 3; γ-H2AX = phosphorylated H2A histone family member X; BCL2 = B-cell lymphoma 2; AMH = anti-Müllerian hormone; FSHR = follicle-stimulating hormone receptor; SASP = senescence-associated secretory phenotype; TME; tumor microenvironment; PDAC = pancreatic ductal adenocarcinoma; AMH = anti-Müllerian hormone; FSHR = follicle-stimulating hormone receptor; DOX = Doxorubicin; ARV825 = BET degrader; I = Irinotecan; Arte = Artesunate; 5-FU = 5-Flourouracil; Leu = Leucovorin; Ator = Atorvastatin calcium; CTX = Cyclophosphamide; Caulerpin = algal metabolite; CRV = Curcuma-derived extracellular vesicles; DR5 = Death Receptor 5 agonist; V,Ven = Venetoclax; Ola = Olaparib; Rosi = Rosiglitazone; Carbo = Carboplatin; D = Dasatinib; Q = Quercetin; MIT = Mitoxantrone; PCC1 = Procyanidin C1; Cis = Cisplatin; ABT-263,Nav = Navitoclax; MMC = Mitomycin C; TFA = Integrin α2β1 ligand peptide; G,GEM = Gemcitabine; A = nab-Paclitaxel (Abraxane); HCW9218 = immune senomodulator; TC = Ganoderma lucidum triterpenoid complex; ABT-737 = BCL-2 inhibitor; S63845 = MCL-1 inhibitor ; DTX = Docetaxel; Eto = Etoposide; NavGal = galacto-navitoclax; EVE = Everolimus; G, GEM = Gemcitabine; TLZ = Talazoparib; Palbo = Palbociclib; Ful = Fulvestrant; GALNP(Nav) = galactose-targeted Navitoclax nanoparticle; Nif =*

Nifuroxazide; NavGal = galactose-modified Navitoclax; Rad = radiation; CTX = Cyclophosphamide; IQ NPs = Quercetin + IR1061 nanoparticles; IR1061 = NIR-II fluorophore.